*Mineralogical Magazine* (2021), **85**, 554–567
doi:10.1180/mgm.2021.50

CAMBRIDGE UNIVERSITY PRESS

**Article – Gregory Yu. Ivanyuk memorial issue**

# Evolution of pyrochlore in carbonatites of the Amba Dongar complex, India.

Shrinivas G. Viladkar[1] and Natalia V. Sorokhtina[2]*

[1]Indian Institute of Science Education and Research Bhopal Department of Earth and Environmental Sciences Bhopal, By-pass Road, Bhauri, Bhopal 462066, India; and [2]Vernadsky Institute of Geochemistry and Analytical Chemistry of the Russian Academy of Sciences, Kosygin Street, 19-1, Moscow 119991, Russian Federation.

**Abstract**

Pyrochlore-group minerals are common accessory rare-metal bearing minerals in the calcite and ankerite carbonatites of the Amba Dongar complex (India). Pyrochlore from the Amba Dongar carbonatites differs from that in other Indian complexes in Ta, Zr, Ti, rare earth element (REE) and Pb contents, but is similar with respect to Ca, Ba and Sr abundances. The evolution of pyrochlore composition was studied to understand the alteration processes and the formation of late-stage pyrochlores enriched in REE and Pb. The early magmatic pyrochlore are calcio- and niobium-dominant types and were replaced by secondary cation-deficient varieties as a consequence of the action of hydrothermal fluids and supergene weathering. These processes produce changes mainly at the *A* site, rarely at the *B* site, and the original F is replaced by $OH^-$ groups. Calcium and Na can be extracted from the structure at the alteration stage and charge balance is achieved by the introduction of REE, Th, U, Ba or Sr. At the latest supergene stages, marginal and fractured zones of pyrochlore grains are altered to Pb-rich, Si-rich and cation-deficient hydrated varieties. The magmatic pyrochlore was crystallised in a highly alkaline environment at a high activity of Ca and at temperatures near 600°C, the alteration of pyrochlore began in a hydrothermal environment at temperatures below 350°C. The major compositional changes that are associated with the alteration are summarised by the following reactions: $Ca^{2+} + Nb^{5+} \rightarrow REE^{3+} + Ti^{4+}$; $Nb^{5+} + Fe^{3+} \rightarrow Ti^{4+} + Zr^{4+}$; and $2Nb^{5+} + Ca^{2+} \rightarrow Ti^{4+} + Si^{4+} + U^{4+}$.

**Keywords:** pyrochlore, compositional evolution, carbonatite, Amba Dongar, India

(Received 23 September 2020; accepted 28 May 2021; Accepted Manuscript published online: 7 June 2021; Guest Associate Editor: Anatoly Zaitsev)

## Introduction

Pyrochlore-group minerals are common rare-metal accessories of carbonatite intrusions, and are typically present in niobium ores in Indian carbonatite occurrences. More than 25 carbonatite complexes have been reported in India (Fig. 1a). Some of them are characterised by different mineral resources, such as REE, Sr, Ba, Nb and F (Krishnamurthy, 2019). Considerable economic concentrations of pyrochlore are found in the Newania, Sevathur, Sung Valley, and Samchampi carbonatite complexes (Viladkar, 1998; Viladkar and Ghose, 2002; Melluso *et al.*, 2010; Sadiq *et al.*, 2014; Viladkar and Bismayer, 2014; Viladkar *et al.*, 2017; Hoda and Krishnamurthy, 2020; Randive and Meshram, 2020). The Amba Dongar, Sevathur [also known as Sevattur], Koratti, Jogipatti, Samalpatti and Pakkanadu carbonatites are potential targets for locating REE, Nb, U and Th resources (Viladkar, 1981; Viladkar and Bismayer, 2010; Viladkar and Bismayer, 2014; Nagabhushanam *et al.*, 2018). The Amba Dongar carbonatites host significant resources of fluorite, REE, P, Ba, Sr and Nb (Palmer and Williams-Jones, 1996; Nanda *et al.*, 2017; Nagabhushanam *et al.*, 2018). Exploration of the Amba Dongar carbonatites has indicated homogeneous mineralisation down to the explored vertical depth of 120–200 m in calcite and ankerite carbonatites, and also the carbonatite breccia (Krishnamurthy, 2019).

Pyrochlore is a widespread accessory mineral in the calcite and ankerite carbonatites of the Amba Dongar complex (Viladkar and Wimmenauer, 1992; Ghose *et al.*, 1997; Viladkar and Bismayer, 2010; Nanda *et al.*, 2017; Magna *et al.*, 2020). Pyrochlore is a primary magmatic mineral that occurs as an early crystallising phase in the carbonatites (Viladkar and Bismayer, 2010). The composition of pyrochlore is known to be modified by transition from a carbonatite magma to a fluid-rich system at the latest stages of formation of pyrochlore and shows a variety of ionic substitutions involving Nb, Ta, Ti, Zr, Ca, Sr, Ba, Si, U, REE, F, OH and other species (Hogarth, 1989; Lumpkin and Ewing, 1995; Hogarth *et al.*, 2000; Lumpkin, 2001; Bonazzi *et al.*, 2006).

Previous studies of pyrochlore from the Amba-Dongar carbonatites were focused on individual pyrochlore crystals from one type of carbonatite (Viladkar and Wimmenauer, 1992; Viladkar and Bismayer, 2010), or on pyrochlores with a specific composition (Ghose *et al.*, 1997; Magna *et al.*, 2020). The objective of the present study is to summarise the new and exisiting literature data on pyrochlore occurrence and composition in the various carbonatites of the Amba Dongar complex and to compare these data with the available information on pyrochlore-group

*Author for correspondence: Natalia V. Sorokhtina Email: nat_sor@rambler.ru
This paper is part of a thematic set 'Alkaline Rocks' in memory of Dr Gregory Yu. Ivanyuk
**Cite this article:** Viladkar S.G. and Sorokhtina N.V. (2021) Evolution of pyrochlore in carbonatites of the Amba Dongar complex, India.. *Mineralogical Magazine* **85**, 554–567. https://doi.org/10.1180/mgm.2021.50

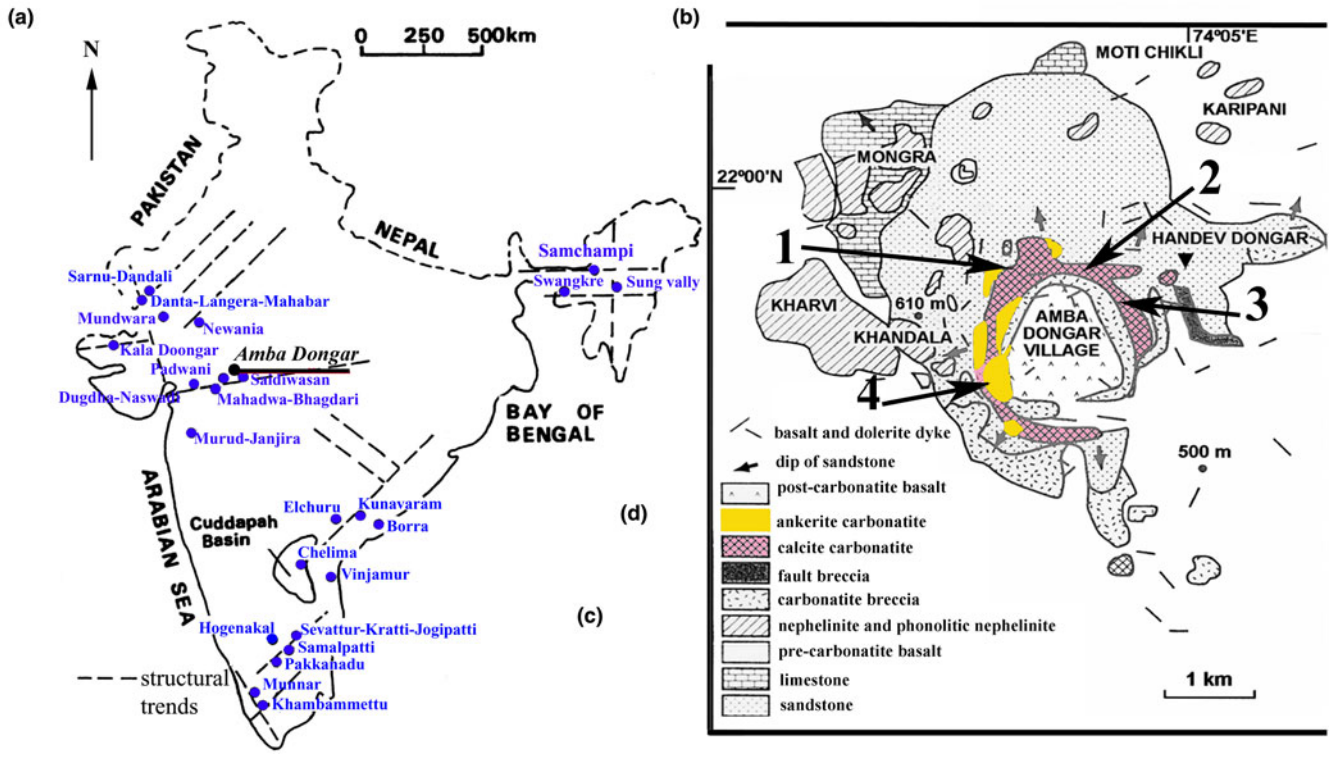


**Fig. 1.** (a) Schematic location map of Indian carbonatite complexes (Krishnamurthy, 2019, reprinted by permission from Springer Nature, COPYRIGHT 2019). (b) Geological map of the Amba Dongar carbonatite complex (Viladkar, 1996, reprinted by permission of the author) with locations of samples investigated: 1–1203; 2–1012; 3–1223; 4–1114.

minerals from other Indian carbonatite complexes. This study also discusses the evolution of pyrochlore composition from the early to late stages of carbonatite formation.

## Geological setting and origin of the carbonatites

Amba Dongar is the largest subvolcanic complex located within the Narmada rift zone ~140 km east of Vadodara, Chhota Udaipur district, Gujarat, India (Fig. 1a). The complex intrudes the Late Cretaceous Bagh sandstone and limestone, and is overlain by the Late Eocene Deccan basalts. The Amba Dongar complex, together with the overlying basalts, fenites and country rocks occupy an area of ~30 $km^2$ (Gwalani *et al.*, 1993; Srivastava, 1997; Viladkar, 1981; 1996; Viladkar and Wimmenauer, 1992). The alkaline and carbonatite magmatism represents a late-stage magmatic event of the Deccan volcanic episode: the U–Pb apatite radiometric ages are 62 ± 22 and 63 ± 19 Ma for carbonatites and 62.3 ± 1.6 Ma for nephelinites (Fosu *et al.*, 2019).

The Amba Dongar complex consists of different generations of calcite and ankerite carbonatites, carbonatite breccia, nephelinite, phonolite and fenitised sandstone (Fig.1b). The carbonatite intrusion hosts a large fluorite hydrothermal deposit. The carbonatite activity commenced with the emplacement of carbonatite breccia and calcite carbonatite. Calcite carbonatite makes up the major part of the intrusion and occurs as a ring dyke collaring an inner rim of carbonatite breccia composed of fragments of calcite carbonatite, gneissic country rock, sandstone, basalt and nephelinite. Calcite carbonatites of the ring dyke were emplaced in several phases. The earlier phase is a coarse-grained calcite carbonatite. These were folllowed by fine-grained calcite carbonatites at a later stage (Viladkar, 1981; Viladkar and Wimmenauer, 1992). Alkaline silicate rocks are represented by nephelinite plugs and a few dykes of phonolite exposed in the peripheral parts of the complex, in low-lying regions around the carbonatite dome. Nephelinite xenoliths are abundant in the calcite carbonatite in the northern part of the ring dyke (Viladkar, 1981, 1996, 2015). The late-stage ankerite carbonatites occur as thin dykes of the first phase and as large plugs of the late phase in the south-western part of the calcite carbonatite ring dyke. The end of carbonatite activity is marked by the formation of hydrothermal fluorite (Deans *et al.*, 1972, 1973; Palmer and Williams-Jones, 1996).

The detailed geology, petrography and mineralogy of the Amba Dongar carbonatites are described in numerous publications (Gwalani *et al.*, 1993; Srivastava, 1997; Viladkar, 1981, 1984, 1996, 2000, 2012, 2015, 2017, 2018; Viladkar and Wimmenauer, 1992; Palmer and Williams-Jones, 1996; Viladkar and Schidlowski, 2000; Doroshkevich *et al.*, 2009). According to these studies, the intrusion was formed in the following sequence: (1) nephelinites and phonolites; (2) carbonatite breccia; (3) coarse-grained calcite carbonatite; (4) fine-grained calcite carbonatite dykes in sandstone, basalts and carbonatite breccia; (5) ankerite carbonatite dykes and plugs within the calcite carbonatites; (6) thin veins of sideritic carbonatite in the ankerite carbonatite; (7) fenitised sandstones; and (8) the final hydrothermal phase of fluorite mineralisation.

Calcite carbonatites are the predominant rock type; and exhibit a wide variation in texture, grain size and colour, which varies from white to brown. The coarse-grained calcite carbonatites occur in different varieties and can be banded, pyroxene-, pyrochlore- or magnetite-rich (Viladkar and Wimmenauer, 1992; Viladkar, 2017; Chandra *et al.*, 2018). The calcite

https://doi.org/10.1180/mgm.2021.50 Published online by Cambridge University Press

carbonatites are formed at magmatic and postmagmatic-hydrothermal stages and consist of primary and secondary minerals. The main primary mineral is calcite, making up to 80 vol.%. Fluorapatite, aegirine–augite, aegirine, phlogopite, magnetite, perovskite, titanite, pyrochlore, zirconolite, columbite and zircon are common accessories, in decreasing order of abundance. Quartz, fluorite, strontianite, Sr-rich baryte, Ba-rich celestine, florencite-(Ce), bastnäsite-(Ce), parisite-(Ce), synchysite-(Ce), monazite-(Ce), ankerite, chalcopyrite, dickite, galena, pyrite, Fe and Mn oxides, ilmenite, vanadinite, wakefieldite-(Ce) and wakefieldite-(La) represent secondary minerals (Viladkar, 1981; Viladkar and Wimmenauer, 1992; Palmer and Williams-Jones, 1996; Srivastava, 1997; Doroshkevich *et al.*, 2009; Magna *et al.*, 2020). According to Doroshkevich *et al.* (2009), the hydrothermal minerals at Amba Dongar were formed by re-equilibration and recrystallisation of the primary carbonatite minerals with a hydrothermal solution. There is evidence that $(OH)^{-}$, $(SO_4)^{2-}$, $F^{-}$, REE, Al and Si were important components of the hydrothermal fluid (Palmer and Williams-Jones, 1996; Williams-Jones and Palmer, 2002; Doroshkevich *et al.*, 2009).

The ankerite carbonatite is a late differentiate of a primary carbonatite magma (Viladkar, 1996; 2018). These carbonatites are dark red in colour and strongly oxidised. Medium- to fine-grained rocks occur in distinct phases. The first phase of ankerite carbonatite intrudes calcite carbonatite, fenite, carbonatite breccia and sandstone. Xenoliths of the calcite carbonatites were digested and metasomatised and contain significant amounts of Fe, Mg, Mn, Sr, Ba and REE (Viladkar and Wimmenauer, 1992). The second-phase ankerite carbonatites form large plugs within the calcite carbonatite ring dyke. All ankerite carbonatites consist predominantly of ankerite with minor proportions of calcite and fluorite, and have a high abundance of REE, in comparison to the calcite carbonatites and carbonatite breccia. The abundance of Ba, Sr, Nb and REE increases from the early to late carbonatite phases. Accessory minerals of the ankerite carbonatites vary in abundance and comprise baryte, hematitised magnetite, apatite, bastnäsite-(Ce), parisite-(Ce), synchysite-(Ce), monazite-(Ce), pyrochlore, quartz, pyrite, galena, chalcopyrite and dickite. Thorite and cerite are not uncommon (Viladkar, 1996; 2018). Phlogopite is observed only in the earlier phase of the ankerite carbonatite. Some samples show intense silicification (Viladkar, 1972). The end of carbonatite activity is marked by the formation of a hydrothermal quartz–fluorite rock (Palmer and Williams-Jones, 1996).

According to isotopic data, the calcite carbonatites are of magmatic origin as their Pb, Rb/Sr, Nd/Sr isotopic ratios are considered to approach mantle values (Simonetti and Bell; Simonetti *et al.*, 1995; Ray *et al.*, 2000). The C and O isotope characteristic of the calcite carbonatites are also consistent with their primary magmatic nature and their trace-element distribution patterns indicate the evolution of these rocks by differentiation of a primary carbonatite melt into initial calcite carbonatites and late-stage calcite carbonatites. The carbonatite magma was initially more magnesian, and this is evident from the presence of phlogopite and periclase in the calcite carbonatite (Viladkar and Wimmenauer, 1992; Viladkar and Schidlowski, 2000; Viladkar, 2012). According to trace-element modelling and petrological constraints, the parental melt that formed the Amba Dongar carbonatite was derived from a metasomatised carbonatised mantle source of garnet lherzolite composition at a depth of >100 km (>3 GPa) aided by $CO_2$-rich fluids and plume-derived heat. The evolutionary transformation of carbonatised silicate magma, concurrent liquid immiscibility, fractional crystallisation, and assimilation, took place at crustal depths (Chandra *et al.*, 2018; Fosu *et al.*, 2019). The ankerite carbonatites are characterised by variation in Pb, C and O isotopic ratios, which are related to fluid activity caused by low-temperature hydrothermal F-rich fluids emanating from the carbonatite magma (Simonetti *et al.*, 1995). Variations in the C–O isotope data and petrographic observations reveal the coupling of fractional crystallisation and post-magmatic fluid–rock interactions to bulk-rock composition. After emplacement, the resetting of clumped isotope signatures in carbonatites is facilitated by post-magmatic processes in both open and closed systems (Fosu *et al.*, 2020). Banerjee and Chakrabarti (2019) found that the calcite and ankerite carbonatites are characterised by geochemical and Ca, Nd and Sr isotopic variations. These are interpreted in terms of crustal contamination, hydrothermal alteration, recycling of ancient subducted carbonates, mantle mineralogy and the depth of magma origin. Mixing calculations suggest that the $\delta^{44/40}$Ca compositions of the Amba Dongar carbonatites reflect up to 20% recycled carbonates in the mantle source.

The temperature regime of hydrothermal fluids for the Amba Dongar carbonatites and fenitised rocks has been studied using primary and pseudo-secondary fluid inclusions hosted by apatite, quartz and fluorite (Deans *et al.*, 1972, 1973; Palmer and Williams-Jones, 1996; Williams-Jones and Palmer, 2002). The results of modelling showed that the intrusion of Ca-rich carbonatite magma and subsequent K–Na metasomatism of the surrounding sandstone were accompanied by separation of aqueous–carbonic fluids containing significant concentrations of Ca, Al and Si. The exsolution of fluids from the carbonatite took place at a temperature of 700°C and a depth of >10 km. The surrounding sandstone was affected by the fluids at temperatures from 400 to 150°C.

## Pyrochlore associations in the carbonatites

Pyrochlore in the Amba Dongar carbonatites has been described by Viladkar (1981) and Viladkar and Wimmenauer (1992). Pyrochlore of early generations are a magmatic accessory phase and occur in variable amounts in all types of carbonatite. In general, pyrochlore is more abundant in the calcite than in ankerite carbonatites (Viladkar and Wimmenauer, 1992; Ghose *et al.*, 1997; Viladkar and Bismayer, 2010; Magna *et al.*, 2020). Recently, it was discovered that the content of this mineral in the calcite carbonatite from the eastern part of the complex can locally reach 50 vol.% and such rocks are composed mainly of pyrochlore, calcite and magnetite (Magna *et al.*, 2020).

Calcite and ankerite carbonatites with pyrochlore mineralisation from different areas of the complex show varied accessory mineralogy. The morphological features of pyrochlore from Amba Dongar are typical for this mineral from intrusive carbonatites (Viladkar and Wimmenauer, 1992; Viladkar, 1996; 2000; Nanda *et al.*, 2017; Magna *et al.*, 2020). Pyrochlore forms individual euhedral grains, octahedral or cubic crystals, and intergrowths of crystals in a carbonate matrix (Fig. 2a–e). The grain sizes vary from 0.02 to 0.4 mm. The colour of pyrochlore ranges from translucent pale golden-yellow to dark brown, and almost opaque (Fig. 2a–c). Pyrochlore from the calcite carbonatites is characterised by a homogeneous texture, with locally a weak blocky and concentric zonation (Fig. 2d–f). The primary magmatic pyrochlore crystallised simultaneously with fluorapatite, and earlier than calcite (Fig. 2d,e). Pyrochlore from the late-stage ankerite

https://doi.org/10.1180/mgm.2021.50 Published online by Cambridge University Press

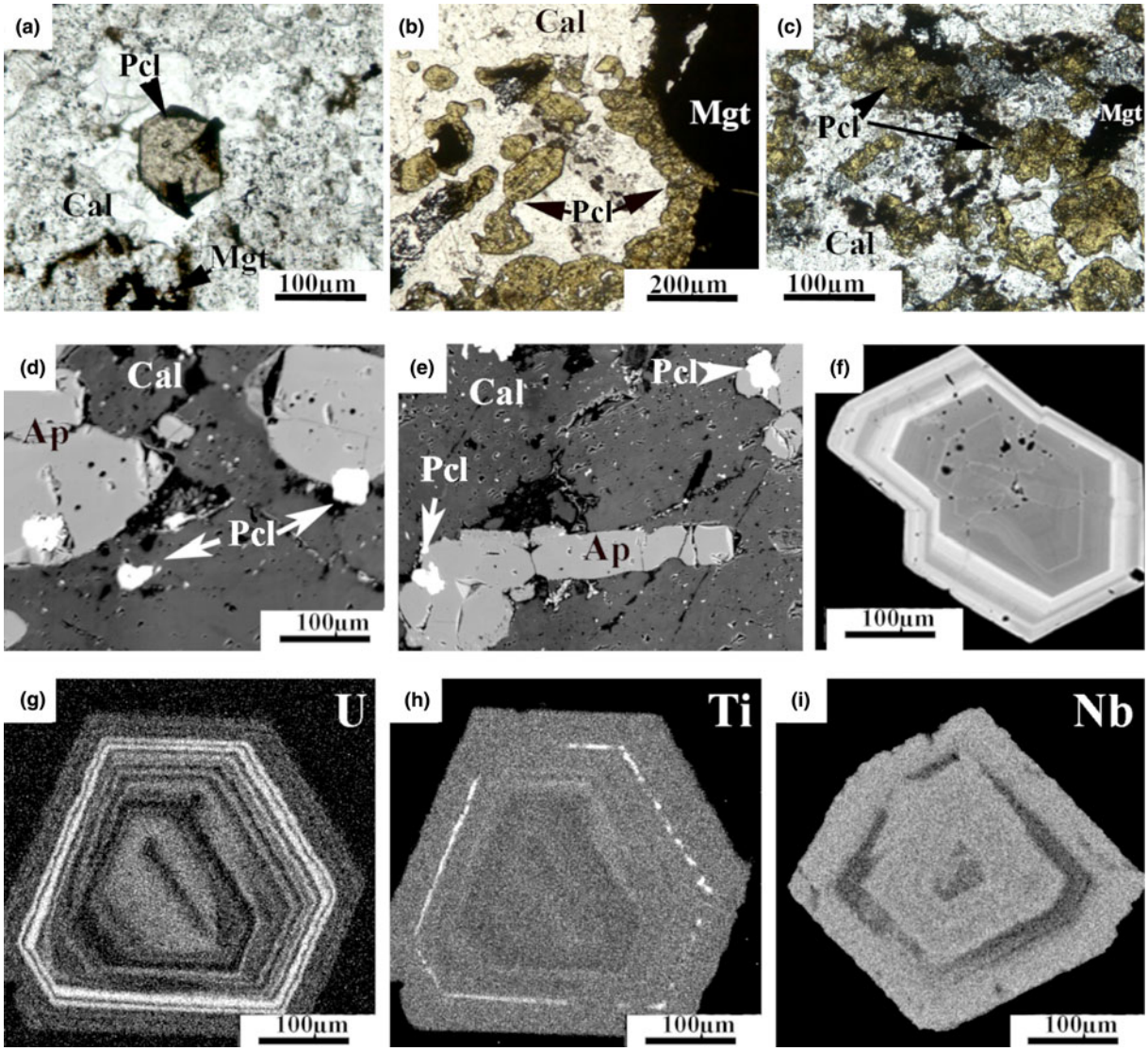


**Fig. 2.** (a–c) Transmitted-light images of calcite (Cal), pyrochlore (Pcl) and magnetite (Mgt) in calcite carbonatites. (d–f) Back-scattered electron images: (d, e) primary fluorapatite (Ap) associated with homogeneous primary pyrochlore from coarse-grained calcite carbonatites; (f) zoned pyrochlore from coarse-grained calcite carbonatite. (g–i) Element maps showing the distribution of U, Ti and Nb in rhythmically zoned pyrochlore from ankerite carbonatites.

carbonatites has distinct repetitive concentric zoning, indicating mechanical disturbance and alteration (Fig. 2g–i). The zoning is very common in large crystals of pyrochlore, which consists of a dark core and a lighter margin. Sometimes pyrochlore in the calcite carbonatite overgrows magnetite (Magna *et al.*, 2020), or occurs as inclusions in large crystals of phlogopite, together with apatite and zircon (Viladkar, 2000). Rarely, phlogopite forms thin bands in association with abundant pyrochlore and Nb-bearing zirconolite, which show a parallel orientation (Viladkar and Wimmenauer, 1992). In some cases, pyrochlore can form discontinuous rims on discrete calcite grains. Large grains of pyrochlore show replacement by calcite together with wakefieldite, baryte and vanadinite (Magna *et al.*, 2020).

## Methods

Pyrochlore in calcite carbonatite thin sections was analysed using a CAMECA SX-100 microprobe at the Mineralogisch-Petrographisches Institute, Hamburg University, Hamburg, Germany. The microprobe was operated at 15 kV accelerating voltage and a beam current of 20 nA. Pyrochlore from ankerite carbonatite (sample 1114) were analysed by electron microprobe analysis (EMPA) using a JEOL JXA 8600 MX Superprobe at the University of Muenster, Germany. This instrument was operated at 20 kV acceleration voltage and a beam current of 15 nA.

The PAP correction procedure was applied to correct for matrix effects. The following standards were used: Nb – Nb metal; F – apatite; Na – jadeite; Si – andradite; Mg – synthetic MgO; Ba – Ba glass; La, Ce and Nd – monazite-Ce; Ta – Ta metal; Ca and Fe – andradite; Sr – synthetic $SrTiO_3$; Zr – synthetic $ZrO_2$; Pb – vanadite; Th – Th glass; U – synthetic $UO_2$; Ti – synthetic $MnTiO_3$. The detection limits do not exceed 0.03 wt.% for most analysed elements and do not exceed 0.05 wt.% for Ta, and 0.1 wt.% for REE, Th, U and F. All the standards were provided by the Smithsonian Institution (National Museum of Natural History), Washington, USA. More detailed information about the standards and applied corrections is available from the analytical laboratories or the authors on request.

https://doi.org/10.1180/mgm.2021.50 Published online by Cambridge University Press

## Terminology of the pyrochlore supergroup

The pyrochlore supergroup is a group of complex cubic oxides, with the general formula $A_{2-m}B_2X_{6-w}Y_{1-n}$ (Hogarth, 1977; Atencio *et al.*, 2010). The *A* site is typically occupied by eightfold-coordinated large cations: $Na^+$, $Ca^{2+}$, $Sr^{2+}$, $Pb^{2+}$, $Sn^{2+}$, $Sb^{3+}$, *REE*$^{3+}$, $U^{4+}$, $Mn^{2+}$, $Ba^{2+}$, $Th^{4+}$, however it can also contain vacancies and $H_2O$. The *B* site is represented by octahedrally coordinated cations: $Nb^{5+}$, $Ta^{5+}$, $Ti^{4+}$, $Sb^{5+}$, $Sn^{4+}$, $Zr^{4+}$, $Hf^{4+}$, $Fe^{3+}$, $Al^{3+}$ and $Si^{4+}$. The *X* site typically is $O^{2-}$ and can include subordinate $(OH)^-$ and $F^-$. The *Y* site hosts $(OH)^-$, $F^-$, $O^{2-}$, vacancies, $H_2O$, or a very large cation ($K^+$, $Cs^+$, $Rb^+$). The symbols *m*, *w* and *n* indicate incomplete occupancy of the *A*, *X* and *Y* sites, respectively. The names of each member of the pyrochlore supergroup are composed of the group name plus two prefixes. The first prefix refers to the dominant cation or anion of the dominant valance or $H_2O$ or a vacancy at the *Y* site: OH – hydroxyl; F – fluor; O – oxy; $H_2O$ – hydro and vacancy – □. The second prefix refers to the dominant cation of the dominant valance or $H_2O$ or a vacancy at the *A* site, e.g. strontio- or natro-. When the first and second prefixes are equal, only one prefix is applied (Atencio *et al.*, 2010).

The pyrochlore supergroup is divided into seven groups on the basis of the atomic proportions of the *B* site cations: pyrochlore group, if Nb is the dominant cation; microlite group (Ta dominant); roméite group (Sb dominant); betafite group (Ti dominant cation); elsmoreite group (W dominant); ralstonite group (Al dominant); and coulsellite group (Mg dominant) (Atencio *et al.*, 2010, 2017; Christy and Atencio, 2013).

Unfortunately, it is impossible to identify pyrochlore-group minerals in a petrological context using this classification as there are no precise electron microprobe analytical methods for the determination of the occupancy of the *X* and *Y* sites or the structural role of the (OH)-group and $H_2O$ (Hogarth, 2013). The correct identification of individual members is possible only if a combination of several advanced analytical techniques is used. Because of these ambiguities, we will use the terminology proposed by Hogarth (1977). Within the pyrochlore subgroups, individual species are named according to the dominant the *A* site cations (Na, Ca, Ba, REE, Pb, U, Th, etc.). A mineral will be referred to simply as pyrochlore, if the contents of Na and/or Ca are dominant and no other large cation exceeds 20% of their total. If the content of any other large cation exceeds 20% of sum of Na and Ca, the species are named on the basis of a dominant large cation in the *A* site (e.g. REE- or Pb-rich pyrochlore).

## Composition of pyrochlore

New data on pyrochlore composition from different types of the Amba Dongar calcite carbonatites (38 analyses for pyrochlore from coarse-grained, banded and pyrochlore-rich carbonatites from the ring dyke) and ankerite carbonatites (132 analyses for different samples from plugs) were obtained in this study (Tables 1, 2). Additionally, pyrochlore compositional data (112 analyses) from previous investigations of the complex were used (Viladkar and Wimmenauer, 1992; Ghose *et al.*, 1997; Viladkar and Bismayer, 2010; Magna *et al.*, 2020). Data from other Indian carbonatite complexes were used for the discussion of pyrochlore compositional evolution: Newania dolomite and dolomite–ankerite carbonatites (Viladkar, 1998; Viladkar and Ghose, 2002; Viladkar *et al.*, 2017); Samchampi calcite carbonatites (Hoda and Krishnamurthy, 2020); Sung Valley (Melluso *et al.*, 2010; Sadiq *et al.*, 2014) and Khamambettu (Burtseva *et al.*, 2013); and Sevathur dolomite carbonatite and its weathered zones (Viladkar and Bismayer, 2014). The evolution of pyrochlore compositions from these Indian carbonatite complexes is presented as binary and ternary plots (Figs 3, 4).

All pyrochlore compositions from the Amba Dongar complex (Tables 1, 2; Fig. 3a) correspond to members of the pyrochlore group. Their composition varies in the calcite and ankerite carbonatites. Most pyrochlore in the calcite and ankerite carbonatites are characterised by a high $Nb_2O_5$ content, reaching 70.7 wt.% in banded calcite carbonatites and 64.7 wt.% in ankerite carbonatites (Tables 1, 2). In the marginal parts of pyrochlore crystals from the ankerite carbonatites, the content of $Nb_2O_5$ decreases to 47.3 wt.% (Viladkar and Bismayer, 2010). Compared to pyrochlore compositions from other Indian carbonatite complexes, pyrochlore from both carbonatite types at Amba Dongar is characterised by a lower concentration of $Ta_2O_5$ typically $\leq$ 0.5 wt.%, except for the rim of one zoned crystal, where the $Ta_2O_5$ content reaches 12.5 wt.% (Viladkar and Bismayer, 2010). Typically, Nb in the *B* site of Amba Dongar pyrochlores is primarily substituted by Ti (Viladkar and Wimmenauer, 1992; Viladkar and Bismayer, 2010). However, in most pyrochlore samples from different carbonatite complexes of the world the niobium in the *B* site is replaced by Ta and less commonly by Ti (Mackay and Simandl, 2015). The average content of $TiO_2$ in pyrochlore from the calcite carbonatites is ~6 wt.%, and ~9 wt.% in the ankerite carbonatites. Similar variations in Ti content are typical for pyrochlore from other Indian carbonatites (Figs 3a, 4a). It was found that in some pyrochlore the content of $TiO_2$ is extremely high – up to 25.0 wt.% in pyrochlore from the banded calcite carbonatite (Table 1) and up to 29.4 wt.% in the coarse-grained calcite carbonatite (Fig. 4a,b) (Viladkar and Bismayer, 2010). The Ti-enriched parts of pyrochlore grains are accompanied by depletion in Nb, Ca and Na and are located in intermediate zones (Fig. 2h,i). Zirconium, Fe, and Si are common impurities at the *B* site. The maximum content of $ZrO_2$ in zoned pyrochlore is 3.6 wt.% in the calcite carbonatites and 2.6 wt.% in the ankerite carbonatites. According to our (Tables 1, 2) and published data (Viladkar and Bismayer, 2010; Magna *et al.*, 2020) the concentrations of $Fe_2O_3$ range from below detection in unaltered cores to 5.0 wt.% and 3.2 wt.% in grain rims in the calcite and ankerite carbonatites, respectively.

The majority of fresh primary pyrochlore from the calcite and ankerite carbonatites give analytical totals close to 100 wt.%, whereas altered pyrochlore tends to have lower totals, especially in the rim and fractured zones (Tables 1, 2). Altered pyrochlore is characterised by a low total cation content in the *A* sites and by an increase in the concentration of Si in the *B* site. In fresh pyrochlore from the calcite carbonatites the content of $SiO_2$ does not exceed 2.1 wt.% (Ghos *et al.*, 1997); Si can substitute for Nb and Ti in the *B* site. Our data shows a good inverse correlation between Nb and Si (Fig. 4c). A similar correlation has been found in pyrochlore from alkaline rocks of the Narssârssuk complex, Greenland, metasomatites of the Lovozero and carbonatites of the Khibiny complexes, Kola Peninsula, nepheline syenite of the Mariupol massif, Ukraine, carbonatites of the Kerimasi volcano, Tanzania and many other alkaline intrusions (Bonazzi *et al.*, 2006; Chakhmouradian and Mitchell, 2002; Zaitsev *et al.*, 2012; Dumańska-Słowik *et al.*, 2014; Zaitsev *et al.*, 2021). Marginal and fractured parts of zoned pyrochlore from the Amba Dongar ankerite carbonatites are enriched in $SiO_2$ up to 7.4 wt.% (Table 2). Usually these parts of altered pyrochlore are

https://doi.org/10.1180/mgm.2021.50 Published online by Cambridge University Press

**Table 1.** Representative compositions of pyrochlore-group minerals from the Amba Dongar calcite carbonatites.*

| | 1 | 2 | 3 | 4 | 5 | 6 | 7 | 8 | 9 | 10 | 11 | 12 | 13 | 14 | 15 | 16 | 17 | 18 | 19 | 20 |
|---|---|---|---|---|---|---|---|---|---|---|---|---|---|---|---|---|---|---|---|---|
| Wt.% | | | | | | | | | | | | | | | | | | | | |
| $Na_2O$ | 4.72 | 5.25 | 4.22 | 4.67 | 4.50 | 4.91 | 3.12 | 0.19 | 0.04 | 0.08 | 0.34 | | 3.67 | 0.38 | 3.41 | 0.47 | 2.43 | 0.53 | 2.81 | 0.21 |
| $K_2O$ | | | | | | | | | | | | | 0.18 | 0.07 | 0.21 | | 0.17 | 0.06 | 0.15 | 0.05 |
| CaO | 18.94 | 18.60 | 18.58 | 19.30 | 19.82 | 19.03 | 19.71 | 20.85 | 20.33 | 18.48 | 21.64 | 14.15 | 22.16 | 16.40 | 21.32 | 14.76 | 22.72 | 12.93 | 18.86 | 14.62 |
| MnO | | | | | | | | | | | | | | 0.06 | 0.08 | 0.07 | 0.17 | 0.08 | 0.07 | 0.04 |
| SrO | 0.51 | 0.40 | 0.50 | 0.70 | 0.88 | 0.60 | 0.52 | 0.28 | 0.42 | 0.32 | 0.32 | 0.16 | 1.11 | 0.11 | 0.89 | 0.33 | 0.32 | 0.68 | 0.68 | 0.38 |
| BaO | 0.17 | 0.06 | 0.11 | 0.19 | 0.21 | | 0.15 | 0.12 | 0.15 | 0.13 | 0.11 | 0.35 | | | | | | | | |
| PbO | | 0.42 | 0.14 | | | | | 0.68 | 0.40 | 0.57 | 1.04 | 0.07 | | 21.05 | 1.57 | 2.15 | 4.50 | 33.27 | 6.53 | 27.00 |
| $La_2O_3$ | 0.44 | 0.32 | 0.44 | 0.29 | 0.25 | 0.31 | 1.02 | 1.00 | 0.73 | 0.72 | 0.57 | 3.52 | 0.35 | 1.41 | 0.39 | 2.75 | 0.39 | 0.62 | 0.58 | 0.90 |
| $Ce_2O_3$ | 2.21 | 0.74 | 3.25 | 0.66 | 0.51 | 0.59 | 5.72 | 16.09 | 17.92 | 17.98 | 15.17 | 2.60 | 0.79 | 3.41 | 0.82 | 5.98 | 0.81 | 1.36 | 1.21 | 2.79 |
| $Nd_2O_3$ | 0.36 | 0.22 | 0.63 | 0.04 | | 0.08 | 1.13 | 0.53 | 0.37 | 0.37 | 0.34 | 1.10 | 0.12 | 0.87 | 0.18 | 1.26 | 0.10 | 0.27 | 0.23 | 0.28 |
| $Sm_2O_3$ | | | | | | | | | | | | | 0.05 | 0.04 | | 0.19 | | | 0.04 | |
| $ThO_2$ | 0.42 | 0.24 | 1.65 | 0.12 | | 0.14 | 0.14 | 0.09 | 0.14 | | | | 0.21 | 0.14 | 0.25 | 0.30 | 0.40 | 0.11 | 0.28 | 0.24 |
| $UO_2$ | 0.22 | 0.13 | 0.85 | | | | | | 0.27 | | | | | | | 0.10 | | | | |
| MgO | | | | 0.33 | 0.49 | 0.22 | 0.79 | 0.33 | 0.84 | 0.25 | 0.11 | 0.29 | | 0.05 | | 0.38 | 0.09 | 0.24 | 1.11 | 0.06 |
| $Fe_2O_3$ | 0.12 | 0.09 | 0.07 | 0.12 | 0.11 | 0.05 | 0.31 | 3.98 | 3.83 | 3.81 | 1.78 | 0.67 | 0.11 | 3.21 | 0.14 | 3.51 | 0.49 | 1.92 | 0.99 | 3.13 |
| $SiO_2$ | | | | 0.06 | 0.18 | 0.08 | 0.08 | | | 0.10 | | 0.09 | 1.63 | 0.06 | 0.92 | 1.48 | 1.13 | 0.50 | 1.51 | 0.09 |
| $TiO_2$ | 5.38 | 4.98 | 7.13 | 2.96 | 3.34 | 3.18 | 2.76 | 6.40 | 7.60 | 7.68 | 9.30 | 24.99 | 5.56 | 3.86 | 5.42 | 11.24 | 5.24 | 5.55 | 5.12 | 3.58 |
| $ZrO_2$ | 3.19 | 2.46 | 2.03 | | 0.05 | 0.04 | 0.16 | 3.22 | 3.28 | 3.57 | 3.18 | 2.14 | 2.06 | 0.91 | 1.83 | 0.48 | 1.70 | 0.43 | 1.19 | 1.23 |
| $Nb_2O_5$ | 62.15 | 63.95 | 60.35 | 69.73 | 66.98 | 70.66 | 61.44 | 47.89 | 40.45 | 46.15 | 47.58 | 48.45 | 58.67 | 46.36 | 59.00 | 52.47 | 55.67 | 38.48 | 53.80 | 43.01 |
| $Ta_2O_5$ | | 0.12 | 0.08 | | | | | | 0.06 | | | | | | | | | | | 0.07 |
| F | | | | | | | | | | | | | 4.33 | 1.18 | 4.01 | 1.17 | 3.98 | 0.89 | 3.67 | 0.89 |
| Total | 98.86 | 98.03 | 100.11 | 99.18 | 97.36 | 99.83 | 97.06 | 101.72 | 96.94 | 100.33 | 101.56 | 98.98 | 100.96 | 99.52 | 100.48 | 99.12 | 100.31 | 97.95 | 98.87 | 98.60 |
| Total (–O≡F) | 98.86 | 98.03 | 100.11 | 99.18 | 97.36 | 99.83 | 97.06 | 101.72 | 96.94 | 100.33 | 101.56 | 98.98 | 99.14 | 99.02 | 98.80 | 98.63 | 98.64 | 97.58 | 97.32 | 98.23 |
| Atoms per formula unit calculated on the sum of the *B*-site cations equal to 2 | | | | | | | | | | | | | | | | | | | | |
| Na | 0.542 | 0.599 | 0.485 | 0.526 | 0.516 | 0.547 | 0.385 | 0.024 | 0.005 | 0.010 | 0.042 | | 0.426 | 0.055 | 0.404 | 0.049 | 0.298 | 0.085 | 0.334 | 0.032 |
| K | | | | | | | | | | | | | 0.014 | 0.007 | 0.016 | 0.002 | 0.014 | 0.007 | 0.012 | 0.005 |
| Ca | 1.201 | 1.172 | 1.180 | 1.202 | 1.256 | 1.172 | 1.344 | 1.418 | 1.463 | 1.248 | 1.468 | 0.709 | 1.420 | 1.309 | 1.397 | 0.853 | 1.542 | 1.150 | 1.237 | 1.239 |
| Mn | | | | | | | | | | | | | | 0.003 | 0.004 | 0.003 | 0.009 | 0.006 | 0.004 | 0.003 |
| Sr | 0.018 | 0.014 | 0.017 | 0.024 | 0.030 | 0.020 | 0.019 | 0.010 | 0.016 | 0.012 | 0.012 | 0.004 | 0.039 | 0.005 | 0.032 | 0.010 | 0.012 | 0.033 | 0.024 | 0.017 |
| Ba | 0.004 | 0.001 | 0.003 | 0.004 | 0.005 | | 0.004 | 0.003 | 0.004 | 0.003 | 0.003 | 0.006 | | | | | | | | |
| Pb | | 0.007 | 0.002 | | | | | 0.012 | 0.007 | 0.010 | 0.018 | 0.001 | 0.000 | 0.422 | 0.026 | 0.031 | 0.077 | 0.744 | 0.108 | 0.575 |
| La | 0.010 | 0.007 | 0.010 | 0.006 | 0.005 | 0.007 | 0.024 | 0.023 | 0.018 | 0.017 | 0.013 | 0.061 | 0.008 | 0.039 | 0.009 | 0.055 | 0.009 | 0.019 | 0.013 | 0.026 |
| Ce | 0.048 | 0.016 | 0.071 | 0.014 | 0.011 | 0.012 | 0.133 | 0.374 | 0.441 | 0.415 | 0.352 | 0.045 | 0.017 | 0.093 | 0.018 | 0.1180 | 0.019 | 0.041 | 0.027 | 0.081 |
| Nd | 0.008 | 0.005 | 0.013 | 0.001 | | 0.002 | 0.026 | 0.012 | 0.009 | 0.008 | 0.008 | 0.018 | 0.002 | 0.023 | 0.004 | 0.024 | 0.002 | 0.008 | 0.005 | 0.008 |
| Sm | | | | | | | | | | | | | 0.001 | 0.001 | | 0.004 | | | 0.001 | |
| Th | 0.006 | 0.003 | 0.022 | 0.002 | | 0.002 | 0.002 | 0.001 | 0.002 | | | 0.001 | 0.003 | 0.002 | 0.003 | 0.004 | 0.006 | 0.002 | 0.004 | 0.004 |
| U | 0.003 | 0.002 | 0.011 | 0.001 | | 0.001 | 0.001 | | 0.004 | 0.001 | 0.001 | 0.000 | | | | 0.001 | | | | |
| Σ*A* site | 1.840 | 1.826 | 1.814 | 1.780 | 1.823 | 1.763 | 1.938 | 1.877 | 1.969 | 1.724 | 1.917 | 0.845 | 1.930 | 1.959 | 1.913 | 1.154 | 1.988 | 2.095 | 1.769 | 1.990 |
| Mg | | 0.002 | | 0.029 | 0.043 | 0.019 | 0.075 | 0.031 | 0.084 | 0.023 | 0.010 | 0.020 | | 0.005 | 0.002 | 0.030 | 0.008 | 0.030 | 0.101 | 0.007 |
| Fe | 0.006 | 0.004 | 0.003 | 0.005 | 0.005 | 0.002 | 0.015 | 0.190 | 0.194 | 0.181 | 0.085 | 0.023 | 0.005 | 0.180 | 0.006 | 0.142 | 0.023 | 0.120 | 0.046 | 0.186 |
| Si | | 0.002 | 0.002 | 0.003 | 0.011 | 0.004 | 0.005 | | 0.002 | 0.006 | 0.001 | 0.004 | 0.097 | 0.005 | 0.056 | 0.080 | 0.072 | 0.042 | 0.093 | 0.007 |
| Ti | 0.239 | 0.220 | 0.318 | 0.129 | 0.149 | 0.137 | 0.132 | 0.305 | 0.384 | 0.364 | 0.443 | 0.879 | 0.250 | 0.216 | 0.249 | 0.456 | 0.250 | 0.346 | 0.236 | 0.213 |
| Zr | 0.092 | 0.071 | 0.059 | 0.000 | 0.002 | 0.001 | 0.005 | 0.100 | 0.107 | 0.110 | 0.098 | 0.049 | 0.060 | 0.033 | 0.055 | 0.013 | 0.053 | 0.017 | 0.036 | 0.048 |
| Nb | 1.663 | 1.700 | 1.617 | 1.833 | 1.791 | 1.836 | 1.768 | 1.374 | 1.228 | 1.315 | 1.362 | 1.024 | 1.587 | 1.562 | 1.631 | 1.279 | 1.594 | 1.444 | 1.489 | 1.538 |
| Ta | | 0.002 | 0.001 | | | | | | 0.001 | | | | | | | | | | | 0.002 |
| Σ*B* site | 2 | 2 | 2 | 2 | 2 | 2 | 2 | 2 | 2 | 2 | 2 | 2 | 2 | 2 | 2 | 2 | 2 | 2 | 2 | 2 |
| F | | | | | | | | | | | | | 0.820 | 0.279 | 0.775 | 0.200 | 0.797 | 0.234 | 0.711 | 0.222 |

*Blank cells denote values below the EMPA detection limit. 1–3 – sample 1012, 4–7 – sample 1203 from calcite carbonatites, 8–12 – samples from banded calcite carbonatites, 13–20 – zoned crystals from coarse-grained calcite carbonatites (13, 15 – cores, 14, 16 – rims, 17, 19 – dark and 18, 20 – bright phases in inclusions, respectively).

https://doi.org/10.1180/mgm.2021.50 Published online by Cambridge University Press

**Table 2.** Representative compositions of pyrochlore-group minerals from the Amba Dongar ankerite carbonatites.*

| | 1 | 2 | 3 | 4 | 5 | 6 | 7 | 8 | 9 | 10 | 11 | 12 | 13 | 14 | 15 | 16 | 17 | 18 | 19 | 20 | 21 | 22 |
|---|---|---|---|---|---|---|---|---|---|---|---|---|---|---|---|---|---|---|---|---|---|---|
| Wt.% | | | | | | | | | | | | | | | | | | | | | | |
| $Na_2O$ | 0.33 | 4.84 | 0.56 | 0.21 | 4.78 | 1.09 | 5.10 | 0.40 | 0.45 | 6.40 | 6.66 | 6.21 | 6.24 | 0.62 | 2.23 | 3.45 | 1.34 | 0.20 | 0.75 | 5.13 | 6.21 | 6.18 |
| CaO | 9.66 | 18.01 | 10.12 | 8.12 | 18.22 | 11.89 | 18.92 | 9.90 | 10.65 | 20.26 | 19.34 | 19.75 | 19.82 | 10.74 | 13.55 | 14.70 | 12.51 | 10.27 | 9.54 | 19.02 | 20.81 | 19.91 |
| SrO | 4.81 | 0.75 | 3.92 | 3.34 | 0.71 | 2.84 | 0.41 | 3.25 | 3.44 | 0.36 | 0.30 | 0.38 | 0.32 | 3.22 | 2.09 | 1.50 | 2.95 | 5.31 | 1.86 | 0.27 | 0.32 | 0.32 |
| BaO | 2.23 | | 0.60 | 2.13 | | 2.61 | | 2.50 | 3.27 | 0.07 | | | | 2.07 | 1.64 | 1.36 | 2.41 | 2.11 | 2.32 | 0.08 | 0.12 | |
| PbO | 5.41 | 0.88 | 8.62 | | | 7.15 | | 0.14 | 0.38 | 0.21 | 0.17 | 0.14 | 0.15 | 0.13 | 0.27 | 0.25 | 0.35 | 0.38 | 0.23 | 0.09 | 0.18 | 0.19 |
| $La_2O_3$ | 0.43 | 0.17 | 0.24 | 0.14 | 0.25 | 0.29 | 0.12 | 0.14 | | 0.11 | | 0.16 | 0.16 | 0.13 | 0.10 | 0.09 | 0.13 | 0.10 | 0.24 | 0.10 | | 0.16 |
| $Ce_2O_3$ | 1.01 | 1.39 | 1.94 | 1.28 | 1.90 | 2.38 | 0.39 | 0.68 | 1.81 | 0.69 | 0.56 | 1.44 | 1.43 | 1.66 | 1.63 | 1.56 | 1.88 | 1.69 | 2.04 | 0.59 | 0.47 | 1.32 |
| $Nd_2O_3$ | | 0.15 | | | 0.17 | | | | 0.09 | 0.14 | 0.18 | 0.16 | 0.12 | 0.16 | 0.13 | 0.11 | | 0.19 | 0.28 | | | 0.14 |
| $ThO_2$ | 0.49 | 0.75 | 0.50 | 1.44 | 1.30 | 0.79 | 0.13 | 0.97 | 1.07 | 0.98 | 0.67 | 1.19 | 1.39 | 0.73 | 0.87 | 1.19 | 1.21 | 0.99 | 1.30 | 0.60 | 0.60 | 1.55 |
| $UO_2$ | 2.08 | 0.60 | 2.68 | 2.05 | 0.36 | 1.70 | 0.43 | 5.55 | 5.61 | 0.19 | 1.65 | 0.15 | | 2.08 | 3.85 | 2.65 | 4.00 | 4.05 | 2.35 | | | |
| MgO | 0.06 | | 0.06 | 0.08 | | 0.06 | | 0.06 | 0.07 | | | | | 0.06 | 0.05 | 0.04 | 0.05 | 0.05 | 0.05 | | | |
| $Fe_2O_3$ | 2.63 | 0.50 | 2.12 | 1.59 | 0.08 | 1.69 | 0.74 | 2.56 | 2.29 | 0.09 | 0.61 | 0.17 | 0.19 | 1.89 | 2.14 | 1.91 | 2.18 | 3.12 | 1.53 | 0.10 | 0.79 | 0.24 |
| $SiO_2$ | 1.86 | 0.27 | 2.10 | 4.33 | 0.09 | 1.91 | 1.08 | 5.71 | 7.42 | 0.52 | 1.53 | 0.10 | 0.07 | 3.96 | 4.57 | 2.95 | 4.14 | 3.16 | 3.41 | 2.21 | 0.46 | |
| $TiO_2$ | 7.96 | 8.34 | 8.38 | 12.27 | 8.68 | 7.69 | 7.98 | 11.07 | 9.35 | 8.28 | 8.10 | 7.51 | 7.42 | 12.62 | 12.24 | 13.30 | 9.61 | 9.15 | 11.68 | 7.88 | 8.92 | 8.22 |
| $ZrO_2$ | 0.42 | 0.84 | 0.61 | 2.57 | 1.06 | 0.87 | 1.82 | 2.12 | | | | | | | | | | | | | | |
| $Nb_2O_5$ | 57.26 | 64.41 | 55.80 | 59.84 | 63.95 | 56.35 | 64.00 | 50.08 | 50.18 | 60.67 | 57.94 | 59.75 | 59.53 | 54.02 | 50.40 | 54.07 | 52.50 | 53.00 | 54.10 | 58.29 | 59.11 | 59.54 |
| $Ta_2O_5$ | 0.32 | 0.08 | 0.05 | 0.28 | | 0.16 | 0.22 | 0.42 | | | | | | | | | | | | | | |
| Total | 96.96 | 101.98 | 98.30 | 99.67 | 101.55 | 99.47 | 101.34 | 95.55 | 96.21 | 99.10 | 97.93 | 97.29 | 97.01 | 94.17 | 95.90 | 99.21 | 95.38 | 93.91 | 91.82 | 94.53 | 98.29 | 97.99 |
| Atoms per formula unit calculated on the sum of the *B*-site cations equal to 2 | | | | | | | | | | | | | | | | | | | | | | |
| Na | 0.035 | 0.515 | 0.061 | 0.019 | 0.513 | 0.121 | 0.527 | 0.039 | 0.045 | 0.725 | 0.753 | 0.732 | 0.739 | 0.061 | 0.226 | 0.344 | 0.141 | 0.022 | 0.076 | 0.575 | 0.697 | 0.720 |
| Ca | 0.574 | 1.058 | 0.609 | 0.402 | 1.081 | 0.728 | 1.081 | 0.532 | 0.586 | 1.267 | 1.209 | 1.286 | 1.298 | 0.584 | 0.759 | 0.810 | 0.728 | 0.604 | 0.540 | 1.178 | 1.291 | 1.281 |
| Sr | 0.155 | 0.024 | 0.128 | 0.090 | 0.023 | 0.094 | 0.013 | 0.095 | 0.102 | 0.012 | 0.010 | 0.013 | 0.011 | 0.095 | 0.063 | 0.045 | 0.093 | 0.169 | 0.057 | 0.009 | 0.011 | 0.011 |
| Ba | 0.048 | 0.000 | 0.013 | 0.039 | | 0.058 | | 0.049 | 0.066 | 0.002 | | | | 0.041 | 0.034 | 0.027 | 0.051 | 0.045 | 0.048 | 0.002 | 0.003 | |
| Pb | 0.081 | 0.013 | 0.131 | 0.000 | 0.000 | 0.110 | | 0.002 | 0.005 | 0.003 | 0.003 | 0.002 | 0.002 | 0.002 | 0.004 | 0.003 | 0.005 | 0.006 | 0.003 | 0.001 | 0.003 | 0.003 |
| La | 0.009 | 0.003 | 0.005 | 0.002 | 0.005 | 0.006 | 0.002 | 0.003 | | 0.002 | | 0.003 | 0.003 | 0.002 | 0.002 | 0.002 | 0.003 | 0.002 | 0.005 | 0.002 | | 0.004 |
| Ce | 0.020 | 0.028 | 0.040 | 0.022 | 0.039 | 0.050 | 0.008 | 0.012 | 0.034 | 0.015 | 0.012 | 0.032 | 0.032 | 0.031 | 0.031 | 0.029 | 0.037 | 0.034 | 0.039 | 0.012 | 0.010 | 0.029 |
| Nd | | 0.003 | | | 0.003 | | | | 0.002 | 0.003 | 0.004 | 0.003 | 0.003 | 0.003 | 0.002 | 0.002 | | 0.004 | 0.005 | | | 0.003 |
| U | 0.026 | 0.007 | 0.033 | 0.021 | 0.004 | 0.022 | 0.005 | 0.062 | 0.064 | 0.002 | 0.021 | 0.002 | | 0.024 | 0.045 | 0.030 | 0.048 | 0.049 | 0.028 | | | |
| Th | 0.006 | 0.009 | 0.006 | 0.015 | 0.016 | 0.010 | 0.002 | 0.011 | 0.012 | 0.013 | 0.009 | 0.016 | 0.019 | 0.008 | 0.010 | 0.014 | 0.015 | 0.012 | 0.016 | 0.008 | 0.008 | 0.021 |
| *A* site | 0.954 | 1.660 | 1.026 | 0.610 | 1.684 | 1.199 | 1.638 | 0.805 | 0.916 | 2.044 | 2.021 | 2.089 | 2.107 | 0.851 | 1.176 | 1.306 | 1.121 | 0.947 | 0.817 | 1.787 | 2.023 | 2.072 |
| Nb | 1.434 | 1.597 | 1.416 | 1.251 | 1.602 | 1.456 | 1.542 | 1.136 | 1.164 | 1.601 | 1.528 | 1.643 | 1.645 | 1.240 | 1.191 | 1.257 | 1.289 | 1.316 | 1.292 | 1.524 | 1.550 | 1.617 |
| Ta | 0.005 | 0.001 | 0.001 | 0.004 | | 0.002 | 0.003 | 0.006 | | | | | 0.001 | | | | | | | | | |
| Ti | 0.332 | 0.344 | 0.354 | 0.427 | 0.362 | 0.330 | 0.320 | 0.418 | 0.361 | 0.364 | 0.355 | 0.343 | 0.341 | 0.482 | 0.481 | 0.514 | 0.393 | 0.378 | 0.464 | 0.343 | 0.389 | 0.371 |
| Zr | 0.011 | 0.022 | 0.017 | 0.058 | 0.029 | 0.024 | 0.047 | 0.052 | | | | | | | | | | | | | | |
| Fe | 0.110 | 0.021 | 0.090 | 0.055 | 0.003 | 0.073 | 0.030 | 0.097 | 0.088 | 0.004 | 0.027 | 0.008 | 0.009 | 0.072 | 0.084 | 0.074 | 0.089 | 0.129 | 0.061 | 0.004 | 0.034 | 0.011 |
| Mg | 0.005 | 0.000 | 0.005 | 0.006 | 0.000 | 0.005 | | 0.004 | 0.006 | | | | | 0.004 | 0.004 | 0.003 | 0.004 | 0.004 | 0.004 | | | |
| Si | 0.103 | 0.015 | 0.118 | 0.200 | 0.005 | 0.109 | 0.058 | 0.287 | 0.381 | 0.031 | 0.089 | 0.006 | 0.004 | 0.201 | 0.239 | 0.152 | 0.225 | 0.174 | 0.180 | 0.128 | 0.027 | |
| *B* site | 2 | 2 | 2 | 2 | 2 | 2 | 2 | 2 | 2 | 2 | 2 | 2 | 2 | 2 | 2 | 2 | 2 | 2 | 2 | 2 | 2 | 2 |

*Blank cells denote values below the EMPA detection limit. The values of F are below the EMPA detection limit. 1–8 – sample 1114, 9–22 – different samples from ankerite plugs, $ZrO_2$ is not defined.

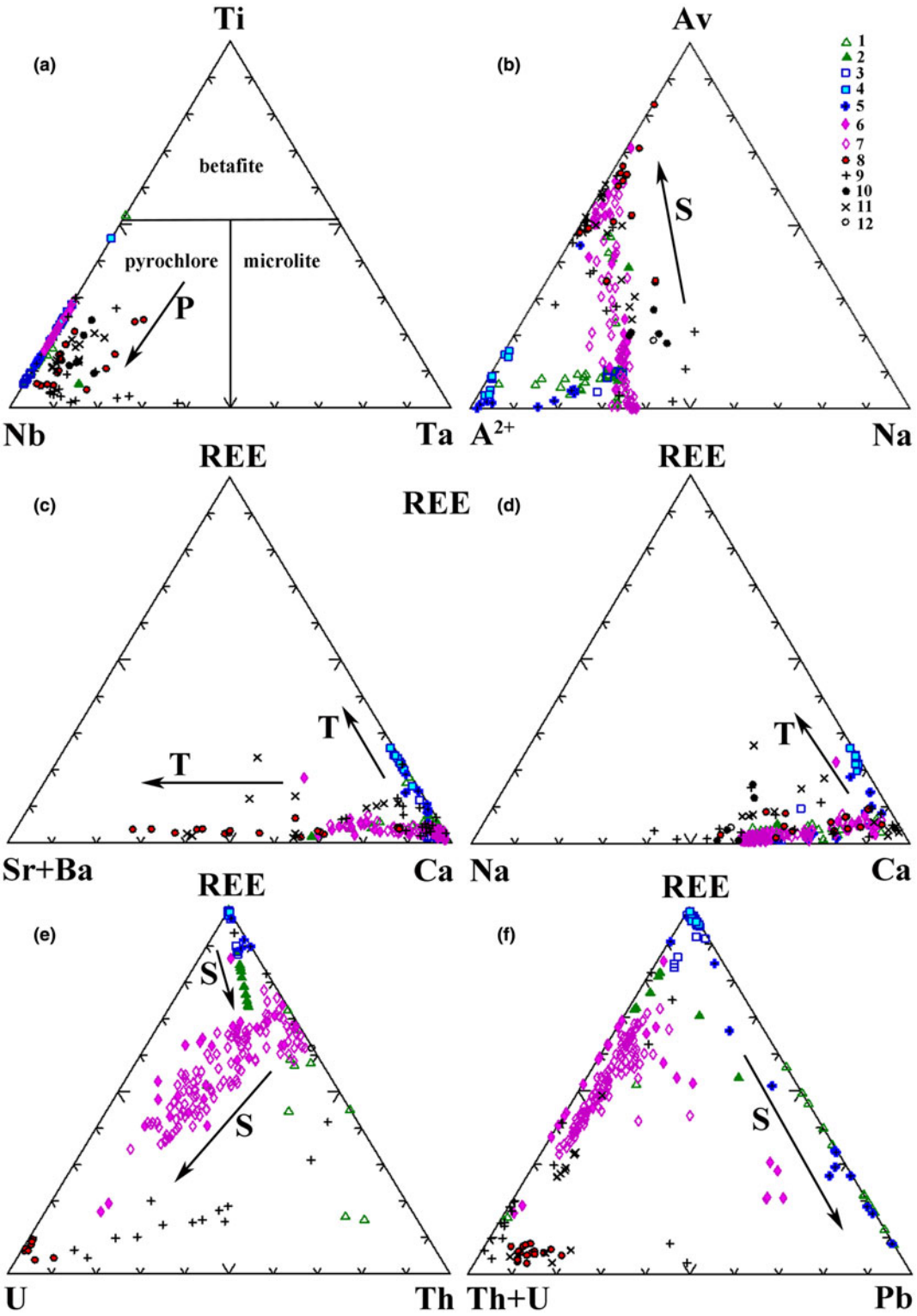


**Fig. 3.** Composition (apfu) of pyrochlore from Indian carbonatite complexes in terms of cation occupancy in (a) the *B* site and (b–f) the *A* site (Hogarth, 1977; Atencio *et al.*, 2010; Lumpkin and Ewing, 1995). (a) Fields of different pyrochlore-group mineral species are shown. (b) The triangle corners are Av – *A*-site vacancy, $A^{2+}$ – sum of divalent cations in the *A* site and Na. Compositional variation of pyrochlore from the Amba Dongar carbonatites is shown as arrows pointing towards progressively more altered compositions: P – primary, T – transitional and S – secondary. The symbols for samples from the Amba Dongar (1–7) and other Indian carbonatite complexes (8–12) are: 1 – coarse-grained calcite carbonatites in samples 1272, 195, 1231, 1223 (Viladkar and Wimmenauer, 1992; Ghose *et al.*, 1997; Viladkar and Bismayer, 2010; Magna *et al.*, 2020); 2 – coarse-grained calcite carbonatite in sample 1012; 3 – coarse-grained calcite carbonatite in sample 1203 (our data and Viladkar and Bismayer, 2010); 4 – banded and 5 – pyrochlore-rich variety of coarse-grained calcite carbonatites from the ring dyke in samples AD-1 and V-1, respectively (our data); 6 – ankerite carbonatite in sample 1114 (our data and Viladkar and Bismayer, 2010); 7 – ankerite carbonatites from different locations in the large plug (our data); 8 – Newania dolomite–ankerite carbonatites (Viladkar, 1998; Viladkar and Ghose, 2002; Viladkar *et al.*, 2017); 9 – Sung Valley calcite carbonatites (Melluso *et al.*, 2010; Sadiq *et al.*, 2014); 10 – Khamambettu calcite carbonatites (Burtseva *et al.*, 2013); 11 – Sevathur dolomite carbonatite (Viladkar and Bismayer, 2014); 12 – Samchampi calcite carbonatites (Hoda and Krishnamurthy, 2020).

https://doi.org/10.1180/mgm.2021.50 Published online by Cambridge University Press

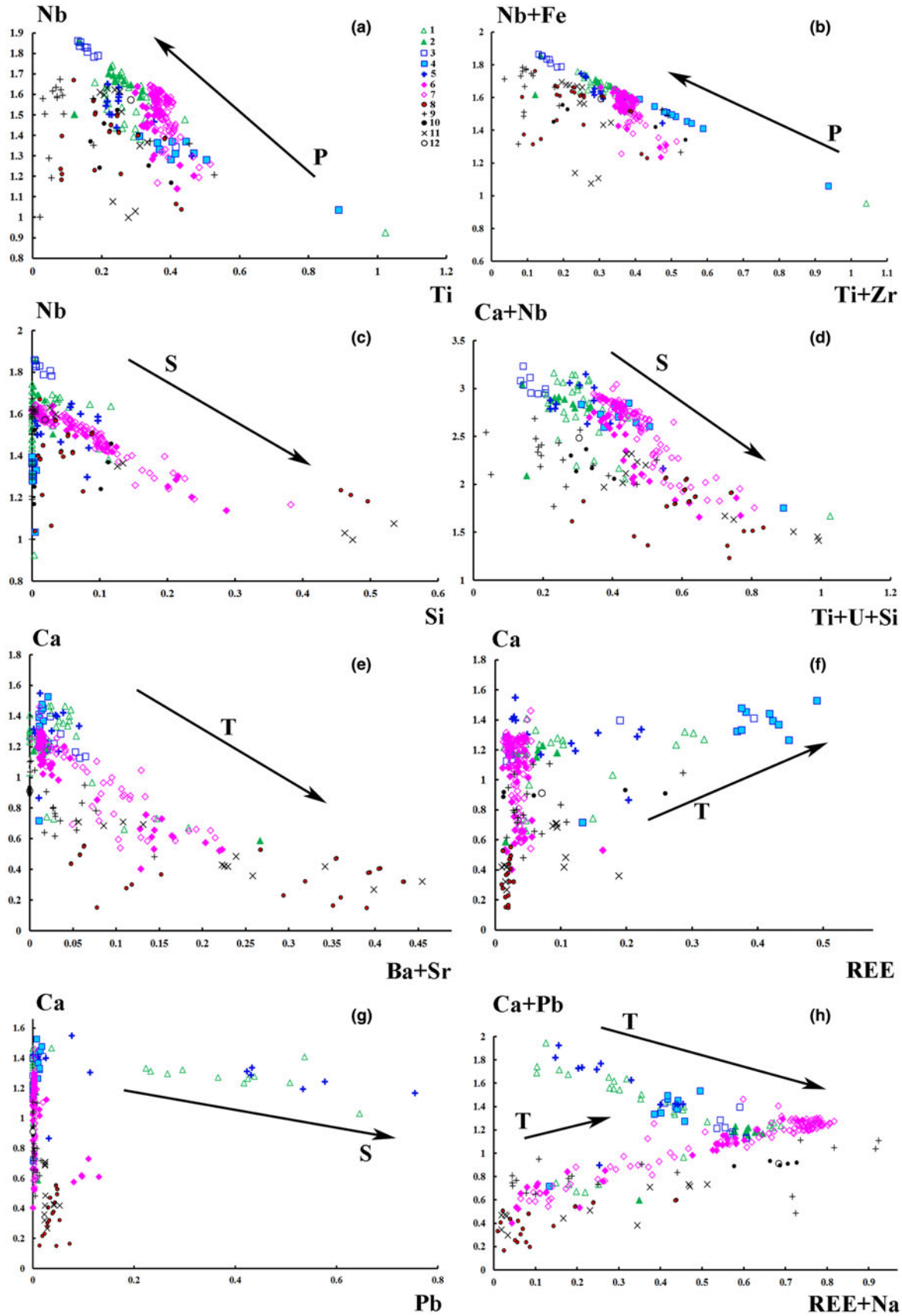


**Fig. 4.** Correlations between the *A*- and the *B*-site cation populations (apfu) in pyrochlore from diverset Indian carbonatites. Compositional variations of pyrochlore from the Amba Dongar carbonatites are shown as arrows pointing towards the progressively more altered compositions: P – primary, T – transitional and S – secondary. The symbols are as in Fig. 3.

https://doi.org/10.1180/mgm.2021.50 Published online by Cambridge University Press

characterised by a deficit of cations at the *A* site and an increased content of uranium (Fig. 4d). Silica could be present in an amorphous or dispersed state, as was argued for Sr-rich pyrochlore from alkaline rocks of the Lovozero complex (Voloshin *et al.*, 1989). Strong enrichment in $SiO_2$ (up to 20.4 wt.%) was found in the altered marginal part of one pyrochlore from the ankerite carbonatites. In addition, this Si-rich area has a high content of CaO, $Nb_2O_5$ and $TiO_2$ (up to 15.7 wt.%, 40.3 wt.% and 6.4 wt.%, respectively). The concentration of $Na_2O$ and $REE_2O_3$ in the alteration zone does not exceed 1 wt.%. It is possible that the high measured Si content arises from the presence of an unidentified silicate phase in the altered area. Given its low Na content and the predominance of Nb over Ti, the most probable contaminant phases are niocalite $(Ca,Nb)_4(Si_2O_7)(O,OH,F)_2$ and mongolite $Ca_4Nb_6Si_5O_{24}(OH)_{10}{\cdot}n(H_2O)$ (Nickel, 1956; Vladykin *et al.*, 1985).

Pyrochlore from the ankerite carbonatites displays more significant cation and vacancy variations in the *A* site than that from the calcite carbonatites (Tables 1, 2). The lowest recorded *A*-site occupancy in pyrochlore from the calcite carbonatites and ankerite carbonatites is 0.88 and 0.62 apfu, respectively. This cation loss is due to the leaching, mainly of Ca and Na during hydrothermal alteration. The contents of CaO and $Na_2O$ in pyrochlore from the calcite carbonatites decrease from 23.0 wt.% (Magna *et al.*, 2020) to 14.2 wt.% and from 5.5 wt.% (Ghos *et al.*, 1997) to below detection, respectively. The contents of CaO and $Na_2O$ in pyrochlore from the ankerite carbonatites range from 20.8 wt.% (Viladkar and Bismayer, 2010) to 9.5 wt.% and from 6.7 wt.% to 0.2 wt.%, respectively (Table 2). Compared to the composition of the pyrochlore-group minerals from other Indian carbonatites, the *A* site of pyrochlore from Amba Dongar is predominantly occupied by divalent cations (Fig. 3b).

The average content of minor and trace elements in pyrochlore from the Amba Dongar calcite and ankerite carbonatites does not exceed 0.4 and 0.1 apfu, respectively. The average content of REE in the pyrochlore from the Amba Dongar calcite carbonatites is higher than in pyrochlore from other Indian carbonatites. Significant contents of $Ce_2O_3$ and PbO (up to 18.0 wt.% and 33.3 wt.%, respectively) have been observed in alteration zones and rims of pyrochlore in the calcite carbonatites (Table 1, Figs 3c–f, 4f–h). According to literature data, Pb-rich pyrochlore is formed as secondary or late generation phase, and has been described from alkaline granites and laterite weathering crusts on carbonatites (Lottermoser and England, 1988; Kartashov *et al.*, 1992; Li *et al.*, 2020).

Viladkar and Wimmenauer (1992) identified pyrochlore from two coarse-grained calcite carbonatite samples from Amba Dongar that showed significant concentrations of $ThO_2$ (up to 15.3 wt.%). Typically the contents of $UO_2$ and $ThO_2$ in pyrochlore from the calcite carbonatites do not exceed 0.3 wt.%, whereas in strongly zoned pyrochlore from the ankerite carbonatites these elements reach 0.9 and 1.2 wt.%, respectively. Primary magmatic pyrochlore contains insignificant amounts of Th and U. The high levels of $UO_2$ (up to 5.6 wt.%) in pyrochlore from the ankerite carbonatites are accompanied by an increase in silica and a significant cation deficit in the *A* site (Table 2, Fig. 4d). The contents of BaO and SrO in pyrochlore from the calcite carbonatites rarely exceed 1 wt.% (Table 1), while rim zones of pyrochlores from the ankerite carbonatites were found to contain up to 3.3 wt.% BaO and 6.2 wt.% SrO (Viladkar and Bismayer, 2010). In general, the average total concentration of Sr and Ba is much lower than in pyrochlore from Newania dolomite–ankerite carbonatite (Viladkar, 1998; Viladkar and Ghose, 2002; Viladkar *et al.*, 2017) and pyrochlore from dolomite carbonatite of Sevathur (Viladkar and Bismayer, 2014) (Figs 3c, 4e).

Of the anions, only fluorine was analysed; this being present in concentrations ranging from below the detection limit to 4.3 wt.% in central zones of pyrochlore grains from the coarse-grained calcite carbonatites (Table 1). Fluorine concentration in pyrochlore from the ankerite carbonatites does not exceed the detection limit.

## Discussion: compositional evolution of pyrochlore in carbonatites

The pyrochlore-group minerals are stable in a wide range of physical and chemical conditions from magmatic to hypergene (Hogarth, 1989; Lumpkin and Ewing, 1995; Lumpkin, 2001; Nasraoui *et al.*, 1999; Nasraoui and Bilal, 2000; Zurevinski and Mitchell, 2004). The compositional evolution and heterogeneity of pyrochlore reflects changes in temperature, redox potential and chemical activities. Variations in cation and anion composition are typical of pyrochlore from intrusive carbonatites and have been studied, for example, at Oka and Aley in Canada, at Khibiny, Lovozero, Kovdor, Vuoriyarvi and Seblyavr in Russia and in Sokli in Finland (Hogarth, 1989; Hogarth *et al.*, 2000; Subbotin and Subbotina, 2000; Chakhmouradian and Mitchell, 2002; Chakhmouradian and Williams, 2004; Chakhmouradian *et al.*, 2015; Zurevinski and Mitchell, 2004; Zaitsev *et al.*, 2012; Lee *et al.*, 2006; Ivanyuk *et al.*, 2018).

Primary pyrochlore crystallised in the early stages of carbonatite formation displays compositional variations mainly in *B*-site cations. There are also significant variations in terms of Ca and U in the *A* site. Pyrochlore precipitated at late hydrothermal stages varies considerably in terms of cation occupancy at the *A* site, and is characterised by cation and anion leaching from the *A*, *X* and *Y* sites and incorporation of $H_2O$ in the structure (Hogarth, 1989; Lumpkin and Ewing, 1995; Nasraoui and Bilal, 2000; Zurevinski and Mitchell, 2004). Apparently, hydration is followed by cation exchange and controlled by diffusion through a stable $B_2X_6$ framework (Geisler *et al.*, 2005).

The alteration of pyrochlore from carbonatite complexes is described by typical substitutions: $A^{2+}O \rightarrow AVXV$, $A^{2+}O \rightarrow AVYV$, and $A^{+}YF^{-} \rightarrow AVYV$, where *V* represents the *A*-, *X*- or *Y*-site vacancy, respectively (Lumpkin and Ewing 1995, Lumpkin 2001; Hogarth, 1989).

Three alteration trends can be distinguished in pyrochlore-group minerals from carbonatites: (1) primary, including magmatic growth, followed by hydrothermal high-temperature alteration (from 600 to 400°C); (2) transitional (hydrothermal alteration at temperature between 300 and 450°C); and (3) secondary, involving pyrochlore alteration below 150°C (Lumpkin and Ewing, 1995; Lumpkin, 2001).

We compared evolution trends of the Amba Dongar pyrochlore to pyrochlore compositions from other Indian carbonatites and these trends are shown as arrows pointing towards altered compositions on the principal classification and discrimination diagrams (Figs 3, 4). Evolution of pyrochlore-group minerals in the Amba Dongar carbonatites involved primarily an increase in the concentration of Ca and a loss of Na at the *A* site, Nb enrichment in the *B* site, and, in a few individual zoned pyrochlore, an increase in Ti and F contents (Tables 1, 2). According to the nomenclature scheme of Atencio *et al.* (2010), these minerals are oxycalciopyrochlore or fluorcalciopyrochlore. Fluorcalciopyrochlore, which contains high amounts of F and

https://doi.org/10.1180/mgm.2021.50 Published online by Cambridge University Press

Na, was found in the cores of fresh pyrochlore crystals in the calcite carbonatite (Magna *et al.*, 2020). Possible substitutions in the Amba Dongar pyrochlore during the primary stage correspond to the following substitution mechanisms: $Ta^{5+} \rightarrow Nb^{5+}$; $2Nb^{5+} + Ca^{2+} \rightarrow 2Ti^{4+} + U^{4+}$; $2Na^{+} \rightarrow Ca^{2+}$; $Na^{+} + F^{-} \rightarrow Ca^{2+} + O^{2-}$; $F^{-} \rightarrow (OH)^{-}$ (Hogarth, 1989; Lumpkin and Ewing, 1995). As can be seen in Tables 1 and 2, the cores of pyrochlore grains from the ankerite and calcite carbonatites have similar compositions, although pyrochlore from the ankerite carbonatites lacks detectable F. The differentiation of a carbonatite melt from calcite to ankerite carbonatites was studied at Amba Dongar by Viladkar and Wimmenauer (1992) and Viladkar and Schidlowski (2000). We hypothesise that, primary pyrochlore in both carbonatite types crystallised at the magmatic stage and the early varieties of pyrochlore from the calcite carbonatite appear to be from a relatively undifferentiated magma, rich in F. Primary pyrochlore was later altered by hydrothermal fluids of variable composition, which separated from the carbonatite melt at late stages. In addition, a strong negative correlation between Zr, Ti, Fe and Nb contents was found in the Amba Dongar pyrochlore, which implies a coupled substitution such as $Nb^{5+} + Fe^{3+} \rightarrow Ti^{4+} + Zr^{4+}$ (Fig. 4b). Pyrochlore from other Indian carbonatites does not show such a correlation. Perhaps, the extra Nb, Ti and Zr required for substitutions could have been derived by transformation of an early Nb-oxide, for example, zirconolite (Chakhmouradian and Williams, 2004; Kogarko *et al.*, 2009). According to Viladkar and Wimmenauer (1992), zirconolite occurring in Amba Domgar calcite carbonatites is characterised by a high content of $Nb_2O_5$, $TiO_2$ and $ZrO_2$ (up to 10.4 wt.%, 25.1 wt.% and 27.6 wt.%), respectively.

Transitional and secondary alteration is characterised by leaching of Na and F from the *A* and the *Y* sites, respectively (Table 1). The content of Na and F in pyrochlore from the calcite carbonatites decrease at the rim and within fractured zones, together with an incease in the proportion of vacancies (Magna *et al.*, 2020). Cation exchange involving Ba, Sr, REE, U, Th, Pb and Fe also occurs and is accompanied by the removal of Na, Ca and F (Figs. 3c–f; 4d–f). In some cases, pyrochlore-group minerals from Amba Dongar, Khamambettu and Sevathur complexes are REE-rich following the substitutional scheme $2Ca^{2+} \rightarrow Na^{+} + REE^{3+}$ (Figs 3d, 4f). Compared to pyrochlore from other Indian carbonatites, a greater enrichment of Amba Dongar pyrochlore in REE is identified in the banded calcite carbonatite, where Ca and Nb is replaced with REE according to the substituton $Ca^{2+} + Nb^{5+} \rightarrow REE^{3+} + Ti^{4+}$, as was demonstrated for the end-member $(REE)NaTiNbO_6(OH,F)$ from the Niocan and Bond Zone deposits of the Oka complex (Zurevinski and Mitchell, 2004). The concentration of REE in pyrochlore from the ankerite carbonatites increases simultaneously with the concentration of Ba and Sr due to secondary replacement of pyrochlore along grain margins; a common feature of pyrochlore from Indian carbonatites (Fig. 4e). The calcite and ankerite carbonatites of the Amba Dongar complex could be locally enriched in REE (mainly Ce) during differentiation of carbonatite melt (Viladkar and Dulski, 1986; Viladkar and Wimmenauer, 1992). Barium and Sr become enriched in the residual fluid at the hydrothermal stage of carbonatite crystallisation and enter the pyrochlore structure due to cation exchange by secondary alteration.

Finally, hydration and leaching of cations from the *A*, *X* and *Y* sites of the pyrochlore occurs at the latest secondary alteration stage. The cores of the primary Amba Dongar pyrochlore from the calcite carbonatites contain small amounts of Sr, Ba, Si, Al and Zr, whereas the rims and fractured zones have lower Ca, Na and F contents, and elevated concentrations of Si, Pb, U, Th and Fe (Fig. 3e,f). Both U and Si show a positive correlation and were deposited along the rims during hydrothermal reworking. In the intensely zoned pyrochlore from the ankerite carbonatite, rim compositions show a remarkable depletion in Nb, Ca and Na, compensated by enrichment in Si, U, Sr, Ti, Th, Fe and Ba (Fig. 4d). The principal substitution is $2Nb^{5+} + Ca^{2+} \rightarrow Ti^{4+} + Si^{4+} + U^{4+}$. The increase in $SiO_2$ activity in the hydrothermal fluid at the late stages of carbonatite crystallisation is also confirmed by the replacement of pyrochlore by a Ca–Nb silicate (see above). Previously, Viladkar and Wimmenauer (1986) reported a Nb-silicate in the Newania ankerite carbonatites. This general trend towards silicates was also described in Kola carbonatites by Chakhmouradian and Williams (2004).

Our data show two Pb variation trends in the Amba Dongar pyrochlore. A secondary alteration trend was found for Pb-rich pyrochlore in the calcite carbonatites characterised by a weakly negative correlation between Ca and Pb (Fig. 4g), or Ca with Pb and Na with REE (Fig. 4h). A correlation between these components is observed for pyrochlore in the ankerite carbonatites and can be interpreted to have involved cation exchange in the *A* site according to the heterovalent substitution: $Ca^{2+} + Pb^{2+} \rightarrow REE^{3+} + Na^{+}$. The higher Pb content in pyrochlore from the calcite carbonatites can be associated with a local secondary enrichment of the hydrothermal fluid in Pb due to the breakdown of Pb-bearing minerals, such as galena.

## Conclusions

From our observations and data from the literature (Viladkar and Bismayer, 2010; Magna *et al.*, 2020), the petrological and geochemical characteristics of the Amba Dongar calcite and ankerite carbonatites suggest that pyrochlore-group minerals are primary magmatic phases in these rocks. Their extensive compositional variation is due to subsequent post-magmatic and hydrothermal alteration of the host carbonatites.

Pyrochlore-group minerals in the Amba Dongar calcite and ankerite carbonatites show that they are mainly Ca-dominant species, whereas Ce- and Pb-rich species are rare.

Primary Ca-dominant pyrochlore from the calcite and ankerite carbonatites displays variations in the concentration of Ca, Na and, to a lesser extent, REE in the *A* site, Ta, Nb, Ti and Zr in the *B*site, and F in the *Y* site. The composition of the primary pyrochlore varies in response to changes in the the compositon of the parental carbonatite melt.

Pyrochlore-group minerals are susceptible to hydrothermal alteration, leading to the formation of hydrated cation- and anion-deficient pyrochlore with a large proportion of vacancies at the *A* site, together with enrichment in Si, Sr, Ba, Th and REE (Lumpkin and Ewing, 1995; Nasraoui and Bilal, 2000). However, the Amba Dongar pyrochlore is characterised by moderate cation- and anion-deficiencies (Tables 1, 2), whereas the recorded variation in Si, Sr, Ba, Th, U and Pb occurs mainly due to transitional and secondary cationic exchange processes.

Secondary pyrochlore is characterised by *A*-site cation and F deficiency, which can be compensated by the incorporation of $OH^{-}$ or $H_2O$. Concentrations of Ba, Sr, Fe, Pb and Si increase in the altered pyrochlore. Such pyrochlore is formed by reaction of the primary pyrochlore with low-temperature hydrothermal solutions, enriched in alkaline earth elements, and by cation exchange reactions. Enrichment of pyrochlore in divalent cations in the *A* site

https://doi.org/10.1180/mgm.2021.50 Published online by Cambridge University Press

does not depend on cation deficiency, whereas the increase in U and Th contents is coupled with the formation of vacancies at this site. During the latest stages, marginal and fractured zones in pyrochlore grains are altered to Pb-, Si-rich and cation-deficient hydrated varieties. Lead might be derived from hydrothermal solutions as a result of galena decomposition.

The analytical data for pyrochlore-group minerals from Indian carbonatites summarised in this study indicate that pyrochlore from Amba Dongar and other complexes differ in the pattern of variation in Zr, Ti, REE, Si and Pb, but show similar variations in Ba and Sr.

The trends of pyrochlore evolution are associated with the primary, transitional and secondary alteration processes that are represented by the following substitution reactions:

$$Ca^{2+} \rightarrow 2Na^{+};\ 2Ca^{2+} \rightarrow Ba^{2+} + Sr^{2+};\ Ca^{2+} + Nb^{5+} \rightarrow REE^{3+} + Ti^{4+};\ Ca^{2+} \rightarrow Pb^{2+};\ Ca^{2+} + Pb^{2+} \rightarrow REE^{3+} + Na^{+};$$

$$Ta^{5+} \rightarrow Nb^{5+};\ Nb^{5+} + Fe^{3+} \rightarrow Ti^{4+} + Zr^{4+};\ 2Nb^{5+} + Ca^{2+} \rightarrow Ti^{4+} + Si^{4+} + U^{4+}.$$

Evolution of the pyrochlore composition is interpreted as an interaction between the magmatic pyrochlore and a hydrothermal solution emanating from the carbonatite magma. On the basis of the temperature of hydrothermal fluids and pyrochlore crystallisation (Lumpkin and Ewing, 1995; Lumpkin, 2001; Williams-Jones and Palmer, 2002), we believe that the early pyrochlore generations crystallised in a highly alkaline environment at temperatures near 600°C. The secondary alteration of pyrochlore began in a hydrothermal environment with a gradual decrease of pH and the fluid temperatures below 350°C. This process was accompanied by elevated activities of Ba, Sr, U, Th, Fe, Pb and Si in the fluid system.

**Acknowledgments.** This work was funded by Grants – DST RFBR 2019/120 for Indian and RFBR 19-55-45010 for Russian investigations, respectively. S.G. Viladkar is grateful to the Alexander von Humboldt Foundation for the financial support to carry out this work in 2013, to Prof. T. Geisler of Münster University, Germany, for part of the microprobe analytical work on pyrochlore in sample 1114, and to Prof. U. Bismayer of Hamburg University, Germany. We acknowledge Principal Editor Roger Mitchell for his helpful suggestions and comments. The authors express gratitude to the reviewers and Guest Editors Anton Chakhmouradian and Anatoly Zaitsev for constructive comments on the article. We thank K. Walsh for valuable improvements to the paper.

## References

Atencio D., Andrade M.B., Christy A.G., Gieré R. and Kartashov P.M. (2010) The pyrochlore supergroup of minerals: nomenclature. *The Canadian Mineralogist*, **48**, 673–698.

Atencio D., Andrade M.B., Bastos Neto A.C. and Pereira V.P. (2017) Ralstonite renamed hydrokenoralstonite, coulsellite renamed fluornatrocoulsellite, and their incorporation into the pyrochlore supergroup. *The Canadian Mineralogist*, **55**, 115–120.

Banerjee A. and Chakrabarti R. (2019) A geochemical and Nd, Sr and stable Ca isotopic study of carbonatites and associated silicate rocks from the ~65 Ma old Ambadongar carbonatite complex and the Phenai Mata igneous complex, Gujarat, India: implications for crustal contamination, carbonate recycling, hydrothermal alteration and source-mantle mineralogy. *Lithos*, **326–327**, 572–585.

Bonazzi P., Bindi L., Zoppi M., Capitani G.C. and Olmi F. (2006) Single-crystal diffraction and transmission electron microscopy studies of "silicified" pyrochlore from Narssarssuk, Julianehaab district, Greenland. *American Mineralogist*, **91**, 794–801.

Burtseva M.V., Ripp G.S., Doroshkevich A.G., Viladkar S.G. and Varadan R. (2013) Features of mineral and chemical composition of the Khamambettu carbonatites, Tamil Nadu. *Journal Geological Society of India*, **81**, 655–664.

Chakhmouradian A.R. and Mitchell R.H. (2002) New data on pyrochlore- and perovskite-group minerals from the Lovozero alkaline complex, Russia. *European Journal of Mineralogy*, **14**, 821–836.

Chakhmouradian A.R. and Williams C.T. (2004) Mineralogy of high-field-strength elements (Ti, Nb, Zr, Ta, Hf) in phoscoritic and carbonatitic rocks of the Kola Peninsula, Russia. Pp. 293–340 in: *Phoscorites and Carbonatites from Mantle to Mine: the Key Example of the Kola Alkaline Province* (F. Wall and A.N. Zaitsev, editors), Mineralogical Society Series 10, London.

Chakhmouradian A.R, Reguir E.P., Kressall R.D., Crozier J., Pisiak L.K, Sidhu R. and Yang P. (2015) Carbonatite-hosted niobium deposit at Aley, northern British Columbia (Canada): mineralogy, geochemistry and petrogenesis. *Ore Geology Reviews*, **64**, 642–666.

Chandra J., Paul D., Viladkar S.G. and Sensarma S. (2018) Origin of the Amba Dongar carbonatite complex, India and its possible linkage with the Deccan large igneous province. *Geological Society*, London, Special Publications, **463**, 137–169.

Christy A.G. and Atencio D. (2013) Clarification of status of species in the pyrochlore supergroup. *Mineralogical Magazine*, **77**, 13–20.

Deans T., Sukheswala R.N., Sethna S.F. and Viladkar S.G. (1972) Metasomatic feldspar rocks (potash fenites) associated with the fluorite deposits and carbonatites of Amba Dongar, Gujarat, India. *Transactions of the Institution of Mining and Metallurgy*, **81**, B1–B9.

Deans T., Sukheswala R.N., Sethna S.F. and Viladkar S.G. (1973) Discussions and contributions: metasomatic feldspar rocks (potash fenites) associated with the fluorite deposits and carbonatites of Amba Dongar, Gujarat, India. *Transactions of the Institution of Mining and Metallurgy*, **82**, B33–B40.

Doroshkevich A.G., Viladkar S.G., Rip G.S. and Burtseva M.V. (2009) Hydrothermal REE mineralization in the Amba Dongar carbonatite complex, Gujarat, India. *The Canadian Mineralogist*, **47**, 1105–1116.

Dumańska-Słowik M., Pieczka A., Temp G., Olejniczak Z. and Heflik W. (2014) "Silicified" pyrochlore from nepheline syenite (mariupolite) of the Mariupol massif, SE Ukraine: A new insight into the role of silicon in the pyrochlore structure. *American Mineralogist*, **99**, 2008–2017.

Fosu B.R., Ghosh P., Chew D.M. and Viladkar S.G. (2019) Composition and U–Pb ages of apatite in the Amba Dongar carbonatite-alkaline complex, India. *Geological Journal*, **54**, 3438–3454.

Fosu B.R., Ghosh P. and Viladkar S.G. (2020) Clumped isotope geochemistry of carbonatites in the north-western Deccan igneous province: aspects of evolution, post-depositional alteration and mineralization. *Geochimica et Cosmochimica Acta*, **274**, 118–135.

Geisler T., Pöml P., Stephan T., Janssen A. and Putnis A. (2005) Experimental observation of an interface-controlled pseudomorphic replacement reaction in a natural crystalline pyrochlore. *American Mineralogist*, **90**, 1683–1687.

Ghose I., Fialin M., Kienast J.R. and Viladkar S.G. (1997) Low-Th pyrochlore in carbonatite from the Amba Dongar carbonatite-alkaline complex, Gujarat, India. *Neues Jahrbuch für Mineralogie – Monatshefte*, **1**, 34–48.

Gwalani L.G., Rock N.M.S., Chang W.J., Fernandez S., Allégre C.J. and Prinzhofer A. (1993) Alkaline rocks and carbonatites of Amba Dongar and adjacent areas, Deccan igneous province, Gujarat, India: 1. Geology, petrography and petrochemistry. *Mineralogy and Petrology*, **47**, 219–253.

Hoda S.Q. and Krishnamurthy P. (2020) Mineralogy, geochemistry and evolution of carbonatites of Samchampi alkaline complex, Assam, India. *Journal of Applied Geochemistry*, **22**, 31–41.

Hogarth D.D. (1977) Classification and nomenclature of the pyrochlore group. *American Mineralogist*, **62**, 403–410.

Hogarth D.D. (1989) Pyrochlore, apatite and amphibole: distinctive minerals in carbonatite. Pp. 105–148 in *Carbonatites: Genesis and Evolution* (K. Bell, editor). Chapman and Hall, London.

Hogarth D.D. (2013) The pyrochlore group: remarks on nomenclature. *The Canadian Mineralogist*, **51**, 801.

https://doi.org/10.1180/mgm.2021.50 Published online by Cambridge University Press

Hogarth D.D., Williams C.T. and Jones P. (2000) Primary zoning in pyrochlore group minerals from carbonatites. *Mineralogical Magazine*, **64**, 683–697.

Ivanyuk G.Yu., Konopleva N.G., Yakovenchuk V.N., Pakhomovsky Y.A., Panikorovskii T.L., Kalashnikov A.O., Bocharov V.N., Bazai A.A., Mikhailova J.A. and Goryainov P. M. (2018) Three-D mineralogical mapping of the Kovdor phoscorite-carbonatite complex, NW Russia: III. Pyrochlore supergroup minerals. *Minerals*, **8**, 277.

Kartashov P.M., Voloshin A.V. and Pakhomovsky Ya.A. (1992) On plumbopyrochlore from Western Mongólia. *Doklady Akademii Nauk SSSR*, **322**, 1137–1140.

Kogarko L.N., Sorokhtina N.V., Zaitsev V.A. and V.G. Senin (2009) Rare metal mineralization of calcite carbonatites from the Cape Verde archipelago. *Geochemistry International*, **47**, 531–549.

Krishnamurthy P. (2019) Carbonatites of India. *Journal of the Geological Society of India*, **94**, 117–138.

Lee M.J., Lee J.I., Garcia D., Moutte J., Williams C.T., Wall F. and Kim Y. (2006) Pyrochlore chemistry from the Sokli phoscorite-carbonatite complex, Finland: implications for the genesis of phoscorite and carbonatite association. *Geochemical Journal*, **40**, 1–13.

Li T., Li Z., Fan G., Fan H., Zhong J., Jahdali N.S., Qin M., Jehani A.M., Wang F. and Nahdi M.M. (2020) Hydroxyplumbopyrochlore, IMA 2018-145. CNMNC Newsletter 54. *Mineralogical Magazine*, **84**, 359–365, https://doi.org/10.1180/mgm.2020.21

Lottermoser B.G. and England B.M. (1988) Compositional variation in pyrochlores from the Mt Weld carbonatite laterite, Western Australia. *Mineralogy and Petrology*, **38**, 37–51.

Lumpkin G.R. (2001) Alpha-decay damage and aqueous durability of actinide host phases in natural systems. *Neues Neues Jahrbuch für Mineralogie – Monatshefte*, **289**, 136–166.

Lumpkin G.R. and Ewing R.C. (1995) Geochemical alteration of pyrochlore group minerals: Pyrochlore subgroup. *American Mineralogist*, **80**, 732–743.

Mackay D.A.R., Simandl G.J. (2015) Pyrochlore and columbite-tantalite as indicator minerals for specialty metal deposits. *Geochemistry: Exploration, Environment, Analysis*, **15**, 167–178.

Magna T., Viladkar S.G., Rapprich V., Pour O., Hopp J. and Čejková B. (2020) Nb–V-enriched sövites of the northeastern and eastern part of the Amba Dongar carbonatite ring dike, India a reflection of post-emplacement hydrothermal overprint? *Geochemistry*, **80**, 1–11.

Melluso L., Srivastava R.K., Guarino V., Zanetti A. and Sinha A.K. (2010) Mineral compositions and petrogenetic evolution of the ultramafic-alkaline – carbonatitic complex of Sung Valley, Northeastern India. *The Canadian Mineralogist*, **48**, 205–229.

Nagabhushanam B., Durai Raju S., Mundra K.L., Rai S.D., Purohit R.K., Verma M.B. and Nanda L.K. (2018) LREE-Nb mineralization in the south western part of Ambadongar carbonatite complex, Chhota Udepur district, Gujarat, India. *Current Science*, **114**, 1608–1610.

Nanda L.K., Verma M.B., Purohit R.K., Khandelwal M.K., Rai S.D. and Mundra K.L. (2017) LREE and Nb multi-metal potentiality of Amba Dongar carbonatite complex, Chhota Udepur district, Gujarat. Pp. 43–44 in: *International Seminar Carbonatites-Alkaline Rocks and Associated Mineral Deposits* (S.G. Viladkar, R. Duraiswamy and P. Krishnamurthy, editors). Amba Dongar, India.

Nasraoui M. and Bilal E. (2000) Pyrochlores from the Lueshe carbonatite complex (Democratic Republic of Congo): a geochemical record of different alteration stages. *Journal of Asian Earth Sciences*, **18**, 237–251.

Nasraoui M., Bilal E. and Gibert R. (1999) Fresh and weathered pyrochlore studies by Fourier transform infrared spectroscopy coupled with thermal analysis. *Mineralogical Magazine*, **63**, 567–578.

Nickel E.H. (1956) Niocalite – a new calcium niobium silicate mineral. *American Mineralogist*, **41**, 785–786.

Palmer D.A.S. and Williams-Jones A.E. (1996) Genesis of the carbonatite-hosted fluorite deposit at Amba Dongar, India: evidence from fluid inclusions, stable isotopes and whole rock-mineral geochemistry. *Economic Geology*, **91**, 934–950.

Randive K. and Meshram T. (2020) An overview of the carbonatites from the Indian Subcontinent. *Open Geosciences*, **12**, 85–116.

Ray J.S., Trivedi J.R. and Dayal A.M. (2000) Strontium isotope systematics of Amba Dongar and Sung Valley carbonatite-alkaline complexes, India: evidence for liquid immiscibility, crustal contamination and long-lived Rb/Sr enriched mantle sources. *Journal of Asian Earth Sciences*, **18**, 585–594.

Sadiq M., Ranjith A.M. and Umrao R.K. (2014) REE mineralization carbonatites from Sung Valley ultramafic-alkaline-carbonatite complex, Meghalaya, India. *Open Geosciences*, **6**, 457–475.

Simonetti A. and Bell K. (1995) Nd, Pb, and Sr isotope systematics of fluorite at the Amba Dongar carbonatite complex, India: evidence for hydrothermal and crustal fluid mixing. *Economic Geology*, **90**, 2018–2027.

Simonetti A., Bell K. and Viladkar S.G. (1995) Isotopic data from the Amba Dongar carbonatite complex, west-central India: evidence for an enriched mantle source. *Chemical Geology*, **122**, 185–198.

Srivastava R.K. (1997) Petrology, geochemistry and genesis of rift-related carbonatites of Ambadungar, India. *Mineralogy and Petrology*, **61**, 47–66.

Subbotin V.V. and Subbotina G.F. (2000) Minerals of the pyrochlore group in phoscorites and carbonatites of the Kola Peninsula. *Proceedings of the Murmansk State Technical University*, **3**, 273–284.

Viladkar S.G. (1981) The carbonatites of Amba Dongar, Gujarat, India. *Bulletin of the Geological Society of Finland*, **53**, 17–28.

Viladkar S.G. (1984) Alkaline rocks associated with the carbonatites of Amba Dongar, Chhota Udaipur, Gujarat, India. *Indian Mineralogist*, *Sukheswala Volume*, 130–135.

Viladkar S.G. (1996) Geology of the carbonatite-alkalic diatreme of Amba Dongar, Gujarat. Pp. 1–74 in *International Carbonatite Workshop*. Ahmedabad. GMDC Science and Research Centre, India.

Viladkar S.G. (1998) Carbonatite occurrences in Rajasthan, India. *Petrology*, **6**, 272–283.

Viladkar S.G. (2000) Phlogopite as an indicator of magmatic differentiation in the Amba Dongar carbonatite, Gujarat, India. *Neues Jahrbuch für Mineralogie – Monatshefte*, **7**, 302–314.

Viladkar S.G. (2012) Evolution of calciocarbonatite magma: evidence from the sövite and alvikite association in the Amba Dongar Complex. Pp. 485–500 in *Geochemistry – Earth's System Processes* (Panagiotaras D., editor). London, https://doi.org/10.5772/32460

Viladkar S.G. (2015) Mineralogy and geochemistry of fenitized nephelinites of the Amba Dongar complex, Gujarat. *Journal of the Geological Society of India*, **85**, 87–97.

Viladkar S.G. (2017) Pyroxene-sövite in Amba Dongar carbonatite-alkalic complex, Gujarat. *Journal of the Geological Society of India*, **90**, 591–594.

Viladkar S.G. (2018) Ferrocarbonatites in the Amba Dongar diatreme, Gujarat, India. *Journal of the Geological Society of India*, **92**, 141–144.

Viladkar S.G. and Bismayer U. (2010) Compositional variation in pyrochlores of Amba Dongar carbonatite complex, Gujarat. *Journal of the Geological Society of India*, **75**, 495–502.

Viladkar S.G. and Bismayer U. (2014) U-rich pyrochlore from Sevathur carbonatites, Tamil Nadu. *Journal of the Geological Society of India*, **83**, 175–182.

Viladkar S.G. and Dulski P. (1986) Rare earth element abundances in carbonatites, alkaline rocks and fenites of the Amba Dongar complex, Gujarat, India. *Neues Jahrbuch für Mineralogie – Monatshefte*, **1**, 37–48.

Viladkar S.G. and Ghose I. (2002) U-rich pyrochlore in carbonatite of Newania, Rajasthan. *Neues Jahrbuch für Mineralogie – Monatshefte*, **3**, 97–106.

Viladkar S.G. and Schidlowski M. (2000) Carbon and oxygen isotope geochemistry of the Amba Dongar carbonatite complex, Gujarat, India. *Gondwana Research*, **3**(3), 415–424.

Viladkar S.G. and Wimmenauer W. (1986) Mineralogy and geochemistry of the Newania carbonatite-fenite complex, Rajasthan, India. *Neues Jahrbuch für Mineralogie Abhandlungen*, **156**, 1–21.

Viladkar S.G. and Wimmenauer W. (1992) Geochemical and petrological studies on the Amba Dongar carbonatites (Gujarat, India). *Chemie der Erde*, **52**, 277–291.

Viladkar S.G., Bismayer U. and Zietlow P. (2017) Metamict U-rich pyrochlore of Newania carbonatite, Udaipur, Rajasthan. *Journal Geological Society of India*, **89**, 133–138.

Vladykin N.V., Drits V.A., Kovalenko V.I., Dorfman M.D., Malov V.S. and Gorshkov A.I. (1985) The new niobium silicate – mongolite $Ca_4Nb_6[Si_5O_{20}]O_4(OH_{10})\ nH_2O$. *Zapiski Vserossiyskogo Mineralogicheskogo Obshchestva*, **114**, 374–377.

https://doi.org/10.1180/mgm.2021.50 Published online by Cambridge University Press

Voloshin A.V., Pakhomovsky Ya.A., Pusharovsky D.Yu., Nadezhina T.N., Bakhchisaraitsev A.Yu. and Kobyashev Yu.S. (1989) Strontian pyrochlore: composition and crystal structure. *New Data of Mineral*, **36**, 12–24.

Williams-Jones A.E. and Palmer D.A.S. (2002) The evolution of aqueous-carbonic fluids in the Amba Dongar carbonatite, India: implications for fenitisation. *Chemical Geology*, **185**, 283–301.

Zaitsev A.N., Williams C.T., Wall F. and Zolotarev A.A. (2012) Evolution of chemical composition of pyrochlore group minerals from phoscorites and carbonatites of the Khibina alkaline massif. *Geology of Ore Deposits*, **54**, 503–515.

Zaitsev A.N., Spratt J., Shtukenberg A.G., Zolotarev A.A., Britvin S.N., Petrov S.V., Kuptsova A.V. and Antonov A.V. (2021) Oscillatory- and sector-zoned pyrochlore from carbonatites of the Kerimasi volcano, Gregory rift, Tanzania. *Mineralogical Magazine*, **85**, https://doi.org/10.1180/mgm.2020.101

Zurevinski S.E. and Mitchell R.H. (2004) Extreme composition variation in pyrochlore group minerals at the Oka Carbonatite Complex, Québec: evidence of magma mixing? *The Canadian Mineralogist*, **42**, 1159–1168.

https://doi.org/10.1180/mgm.2021.50 Published online by Cambridge University Press